MARMARA UNIVERSITY
FACULTY OF ENGINEERING

PREDICTIVE HVAC SYSTEM FOR CRITICAL ENVIRONMENTAL CONDITIONS

ALİ BERK ALOĞLU

GRADUATION PROJECT REPORT
Department of Mechanical Engineering

Supervisor
Dr. Namık ÜNLÜ

ISTANBUL,2026

MARMARA UNIVERSITY
FACULTY OF ENGINEERING

PREDICTIVE HVAC SYSTEM FOR CRITICAL ENVIRONMENTAL CONDITIONS

BY

ALI BERK ALOĞLU

JANUARY, 2026 ISTANBUL

SUBMITTED TO THE DEPARTMENT OF MECHANICAL ENGINEERING IN PARTIAL FULFILLMENT OF THE REQUIREMENTS FOR THE DEGREE OF

BACHELOR OF SCIENCE

AT

MARMARA UNIVERSITY

Signature of Author(s) .....

Department of Mechanical Engineering

Certified By .....

Project Supervisor, Department of Mechanical Engineering

Accepted By.....

Head of the Department of Mechanical Engineering

ACKNOWLEDGEMENT

First and foremost, I would like to express my sincere gratitude to my supervisor, Dr. Namık Ünlü, for his valuable guidance, constructive suggestions, and the moral support he provided throughout the preparation of this thesis. I am particularly grateful for his encouragement during periods when my motivation as a student declined, as well as for his contributions to the development of my academic vision.

I would also like to sincerely thank Mr. Gökhan Özkan, whom I met during my compulsory internship in the field of mechanical engineering. His knowledge and experience made significant contributions to my professional development, his approach to engineering helped shape my vision, and his guidance and support—both technical and moral—during challenging times inspired me to say, "I want to be an engineer like this." I consider him both an elder brother and a mentor.

Finally, I would like to thank my father; beyond his responsibilities as a parent, he has been a companion throughout my journey, a source of support in difficult times, a friend when I felt alone, and the person who taught me engineering.

January, 2026 Ali Berk Aloğlu

CONTENTS

ABSTRACT

The increasing demand for energy, driven by population growth, urbanization, and the widespread use of Heating, Ventilation, and Air Conditioning (HVAC) systems as major contributors to energy consumption in residential, commercial, and industrial sectors, has intensified the need for energy-efficient solutions to reduce greenhouse gas emissions and improve market competitiveness.

In this study, an MPC-based control solution for HVAC system is implemented through simulation using a hypothetical laboratory environment as a case study. The work begins with an introduction to thermodynamics and heat transfer theory, followed by the development of a thermal model to enable mathematical formulation of the system dynamics. A lumped Resistance–Capacitance (RC) approach is adopted for envelope-based thermal modelling, which is subsequently extended to an aggregated thermal model. The governing differential equations and the corresponding mathematical model are derived based on this aggregated thermal representation.

The proposed predictive control framework is implemented in MATLAB using the Model Predictive Control Toolbox in conjunction with the Control System Toolbox. This implementation enables dynamic modelling, constraint handling, and simulation of a switched linear time-invariant (LTI) HVAC system. The MPC design process starts with the formulation of state-space equations derived from the differential equations and the physical properties of the hypothetical laboratory environment. MPC design parameters are configurable through a graphical user interface (GUI), allowing flexible tuning of controller settings.

The cost function weights are selected to prioritize thermal comfort while simultaneously optimizing energy consumption. Operational constraints are defined via the GUI and incorporated directly into the MPC formulation. Disturbance inputs are obtained from a scenario based on meteorological data corresponding to the month of January in Istanbul.

The inclusion of ventilation effects and air infiltration caused by intermittent door opening introduces time-varying dynamics, which violate the strict LTI assumption. To address this, a switched LTI modelling approach is employed, where the state-space equations are updated at each sampling interval.

Simulation results are presented through graphical analysis of state variables, HVAC control inputs, and selected disturbance parameters. Several test scenarios are evaluated to assess controller behavior, and the obtained results are subsequently analyzed and discussed.

SYMBOLS

T_{in} : Indoor air temperature
T_{out} : Outdoor air temperature
T_{ew} : Exterior wall temperature
T_{iw} : Interior wall temperature
T_f : Floor temperature
T_c : Ceiling temperature
T_m : Internal mass temperature
W_{in} : Indoor humidity ratio
Q_{sens} : Sensible heat transfer rate
Q_{latent} : Latent heat transfer rate
Q_{solar} : Solar heat gain
Q_{HVAC} : HVAC heat input/output
R : Thermal resistance
C : Thermal capacitance
h_c : Convective heat transfer coefficient
h_r : Radiative heat transfer coefficient
A : Heat transfer area
k : Thermal conductivity
L : Thickness of material layer
$\dot{m}$: Mass flow rate of air
c_p : Specific heat capacity of air
h_{fg} : Latent heat of vaporization
$\sigma(t)$: Door opening factor
x(t) : State vector
u(t) : Control input vector
w(t) : Disturbance vector
y(t) : Output vector
Q : Output weighting matrix (MPC)
R : Input weighting matrix (MPC)
S : Input rate weighting matrix (MPC)
N_p : Prediction horizon
N_c : Control horizon
ECR : Error Cost Ratio (slack penalty)

ABBREVIATIONS

HVAC : Heating, Ventilation and Air Conditioning
MPC : Model Predictive Control
RC : Resistance–Capacitance
LTI : Linear Time-Invariant
ZOH : Zero-Order Hold
PID : Proportional–Integral–Derivative
SHGC : Solar Heat Gain Coefficient
ACH : Air Changes per Hour
GUI : Graphical User Interface
ISO : International Organization for Standardization
ASHREA: American Society of Heating, Refrigerating and Air-Conditioning Engineers

LIST OF FIGURES

LIST OF TABLES

1 INTRODUCTION

The limited availability of energy resources, the contribution of fossil-based energy systems to increased greenhouse gas emissions, and the continuous growth in global population and economic activity make the escalation of energy-related challenges a readily foreseeable outcome (Boodi, Beddiar, Amirat, & Benbouzid, 2022), (S, 2012), (Michilidis, Michilidis, Minelli, & Coban, 2025).

In this context, energy conservation can be interpreted not only as a reduction in consumption but also as an indirect contribution to energy production capacity. When the cost of saved energy is lower than the cost of generating additional energy through conventional means, energy-saving technologies become economically and environmentally more valuable.

Consequently, the development and deployment of energy-efficient systems play a critical role in addressing future energy and sustainability challenges.

Heating and cooling represent a significant share of energy consumption in residential, commercial, and industrial sectors. In these domains, thermal comfort requirements are increasingly met through Heating, Ventilation, and Air Conditioning (HVAC) systems.

Consequently, the development of energy efficient HVAC systems has become an important research and engineering focus. Such systems not only facilitate compliance with environmental sustainability standards but also improve market competitiveness by reducing operational energy costs.

Model Predictive Control (MPC) is one of the advanced controls approaches capable of performing dynamic energy management in HVAC systems by explicitly accounting for system dynamics, operational constraints, and future disturbances, thereby enabling improved energy efficiency and reduced energy consumption

In the study by (Michilidis, Michilidis, Minelli, & Coban, 2025) MPC is examined in depth, and various MPC modeling paradigms—including white-, grey-, and black-box approaches—are reported to achieve superior performance compared to rule-based control and other control strategies in terms of energy efficiency and CO_2 emission reductions.

Comparative results related to White-Box MPC, which is necessarily adopted for the study are presented in percentage terms in Table 3 of the reference paper.

The aim of this thesis is to develop and implement a predictive control methodology for HVAC systems, with a specific focus on heating and humidification processes, in order to improve energy efficiency while maintaining indoor thermal comfort. The proposed approach employs predictive modelling to anticipate the thermal and moisture dynamics of the conditioned space, enabling optimized HVAC operation that has the potential to reduce energy consumption and associated emissions.

It should be noted that, although predictive control strategies are widely recognized for their potential to achieve measurable energy savings, the quantitative contribution of the proposed method in terms of energy reduction or emission mitigation is not experimentally evaluated within the scope of this study. Instead, this work focuses on the development, formulation, and implementation of the predictive control framework, providing a methodological foundation for future studies involving performance benchmarking and experimental validation.

This limitation arises from the adoption of a white-box modelling approach based solely on thermodynamics and heat transfer principles, which requires detailed physical properties of the subject building. In contrast to gray-box models that rely on measurement data captured from a test building, or black-box models that depend on historical data, no such data are available for direct comparison in this study.

When developing strategies to minimize energy consumption in buildings, it is essential to understand the dynamic behavior of energy generation and losses. Since building energy processes are inherently time-dependent, their analysis requires a dynamic modelling framework.

The analysis of dynamic energy behavior is fundamentally based on mathematics; however, a mathematical model cannot be established directly without first defining a suitable physical representation of the system. In this context, a thermal model of the building serves as an essential intermediate step, describing heat and moisture transfer mechanisms and enabling the derivation of the corresponding mathematical model.

Thermal building models provide the basis for analyzing building energy demand, indoor thermal comfort, and HVAC system response. Various modelling approaches have been

proposed in the literature, including lumped-parameter models, finite difference and finite element methods, and impulse response–based techniques (S, 2012)

Among these approaches, lumped Resistance–Capacitance (RC) models are widely used due to their simplicity and low computational requirements. Various lumped RC model structures have been proposed in the literature (Tayler & Tarek).In this study, a 2R1C model is selected to represent the building envelope. The overall thermal model is formulated as an aggregated structure composed of envelope elements, doors, windows, and internal thermal mass models.

2 CASE STUDY BUILDING

The hypothetical space considered in the simulation is a laboratory located on the ground floor of an industrial or R&D building (**Figure 2.1**). The laboratory has three exterior-facing walls exposed to the outdoor environment. On the south-facing wall, there is a sealed double-glazed window with no operable opening. Access to the laboratory is provided through a door located on an interior wall that connects the space to the rest of the building.

The spaces adjacent to the laboratory include a basement level below and occupied areas above, consisting of offices or other laboratories. Consequently, heat transfer through the floor and ceiling occurs between conditioned interior zones rather than directly with the outdoor environment.

The laboratory has a rectangular floor plan with dimensions of 8 meters in width and 10 meters in length, and a ceiling height of 3 meters, resulting in a total conditioned volume of 240 m^3.

The laboratory walls, ceiling, and floor are modeled as three-layer composite structures. All physical and thermal properties of the building envelope, including layer compositions, material properties, and thicknesses, are provided in the accompanying ***SimulationTable.xls*** file. The use of an external Excel file enables configurability of the physical parameters and layer definitions, allowing the building structure to be easily modified without altering the simulation model. For this reason, detailed physical properties are not explicitly listed in this document.

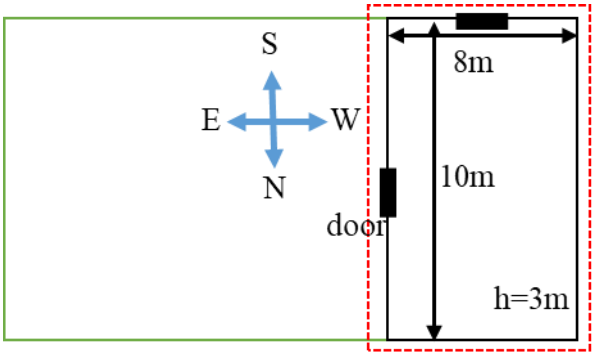

Figure 2-1 Case Study Building Drawing

3 MATHEMATICAL MODELLING OF THE HVAC CONTROLLED SPACE

3.1 Application of the First Law of Thermodynamics to the System

In this project, the following two assumptions are adopted, both of which influence the thermodynamic formulation:

- Open System Assumption

Due to ventilation and infiltration when the door is open even for short time, system becomes open system thermodynamically.

- Rigid Boundary Assumption

The walls, floor, and ceiling are assumed to be rigid, implying that the system volume remains constant ($\Delta V = 0$). Therefore, the system boundary is fixed.

Thermodynamics first law also known as the conversation of energy for an open system can be written as follow (Bergman, 2017), (Çengel, 2020):

$$\Delta E_{st}^{tot} = Q - W + \sum \dot{m}_{in}\left(h + \frac{V^2}{2} + gz\right) - \sum \dot{m}_{in}\left(h + \frac{V^2}{2} + gz\right) \qquad (3.1.1)$$

Where ΔE_{st}^{tot} the change is in the total energy stored in the system, Q is the net heat transferred to the system, and W is the net work done by the system. The summation terms account for the energy transported by mass flow across the system boundaries, where $\dot{m}$ is the mass flow rate, h is the specific enthalpy, V is the flow velocity, g is the gravitational acceleration, and z is the elevation relevance to a reference datum.

If there are energy resources inside the system:

$$\Delta Est = (Qin + Win + Qm\_in + Wm\_in) - (Qout + Wout + Qm\_out + Wm\_out) + Egen \quad (3.1.2)$$

In Equation (3.1.2), the work term Win, Wout is assumed zero due to the presence of a fixed control volume boundary. Furthermore, the kinetic and potential energy contributions, Wm_in, Wm_out, in the mass flow summation terms are neglected, as their effects are considered negligible relative to the thermal energy content of the system. (3.1.2) Equation, assuming Egen is only heat resources, becomes:

$$\Delta E_{st} = Q_{net} = (Q_{in} + Q_{m\_in}) - (Q_{out} + Q_{m\_out}) + Q_{gen} \quad (3.1.3)$$

ΔEst

$$\Delta Est = Q_{net} \quad (3.1.4)$$

If instead of Δt (time interval), we use instant t then:

$$\frac{dE_{st}}{dt} = \frac{dQnet}{dt} \quad (3.1.5)$$

$$\frac{dE_{st}}{dt} = mc\frac{dT}{dt} = C\frac{dT}{dt} \quad (3.1.6)$$

Where:

c is specific heat capacity (J/(kg.K). It is assumed that c ≈ cp ≈ cv (since ΔV≈0)

m is the mass of material (kg)

C is the thermal capacitance (J/K)

$$C\frac{dT}{dt} = \frac{d\,(Q_{in}+Q_{m\_in})-(Q_{out}+Q_{m\_out})+Q_{gen})}{dt} \quad (3.1.7)$$

The heat transfer term Q consists of two components; sensible heat and latent heat. Sensible heat directly affects the temperature of the system and is therefore incorporated into the heat balance equations. In contrast, latent heat does not contribute directly to temperature variation but is associated with phase change processes and is accordingly accounted for in the humidity (moisture) balance equations.

3.2 Heat Transfer Mechanisms and Thermal Load Components

3.2.1 Heat Transfer Mechanisms

3.2.1.1 Conduction

Conduction is the transfer of energy from the more energetic particles of a substance to the adjacent less energetic ones as a result of interactions between the particles. Conduction can take place in solids, liquids, or gases. Energy transfer by conduction occurs in the direction of decreasing temperature.

The Q_{cond} is expressed as:

$$\dot{Q}_{cond} = kA\frac{dT}{dx} = kA\frac{T_{out}-T_{in}}{L} \quad (3.2.1.1.1)$$

Where:

- $\dot{Q}_{cond}$ is the rate of heat transfer by conduction (W)
- A is the heat transfer area (e.g. wall surface area) (m^2)
- T_{out} -T_{in} is the temperature difference across the component (°C)
- k is thermal conductivity of the material (W/m·K)
- L is the thickness of the component (e.g. wall thickness) (m)

Equation (3.2.1.1.1) can be reformulated using an electrical circuit analogy by defining the thermal resistance of the component as

$$R_{cond} = \frac{L}{kA} \text{ (K/W)}$$

Accordingly, the conductive heat transfer rate can be written as

$$\dot{Q}_{cond} = \frac{T_{out}-T_{in}}{R_{cond}}$$

This resistance-based formulation provides a convenient representation for integration into lumped-parameter thermal models and control-oriented building energy simulations.

3.2.1.2 Convection

Convection is the mode of heat transfer between a solid surface and an adjacent fluid (liquid or gas) in motion, involving the combined effects of energy diffusion by conduction and energy transport by fluid motion.

The convective heat transfer rate Q_{conv} is expressed as:

$$\dot{Q}_{conv} = h_c A(T_s - T_\infty) \quad (3.2.1.2.1)$$

Where:

- $\dot{Q}_{conv}$ is the heat transfer rate by convection (W)
- Ts is the surface temperature (e.g. wall surface temperature) (°C).
- T∞ is the temperature of fluid adjacent to the surface (°C)
- hc is convective heat transfer coefficient (W/m2. K)
- A is the heat transfer area (m2)

Equation (3.2.1.2.1) can be reformulated using an electrical circuit analogy by defining the convective thermal resistance of the component (e.g. the outer or inner surface of a wall) as

$R_{conv} = \frac{1}{h_c A}$ (K/W)

Accordingly, the convective heat transfer rate can be written as

$$\dot{Q}_{conv} = \frac{T_s - T_\infty}{R_{conv}} \quad (3.2.1.2.2)$$

Convective heat fluxes directly affect the space air temperature due to the immediate heat exchange between surfaces and the zone air. This is particularly important for evaluating internal heat sources. The total heat gains from lighting, appliances, and equipment consist of two components: convective and radiative. These components are handled separately in the thermal model.

It should be noted that the convective heat transfer coefficient hc is not property of the fluid. Instead, its value depends on flow conditions, surface orientation, and temperature differences. In this study, h_c, is determined in according with (ISO 6. , 2017) standard, as given in **Table 3.1**.

Table 3-1 Values of the Convective Surface Coefficient

Convective surface coefficient	Direction of heat flow		
m^2.K/W	Upwards (*floor*)	Horizontal (*internal wall*)	Downwards (*ceiling*)
$h=h_{ci}$ (internal surfaces)	5,0	2,5	0,7
$h=h_{ce}$ (external surfaces)	$4 + 4.\ v$[1]		

In the simulation studies, the wind speed is assumed constant and equal to 2 m/s.

3.2.1.3 Radiation

Thermal radiation is a form of electromagnetic radiation, distinct from other forms such as X-rays and gamma rays, which is emitted by bodies due to their temperature. All bodies with a temperature above absolute zero emit thermal radiation.

Radiation in emitting is the energy emitted by matter/surface in the form of electromagnetic waves (or photons) as a result of the changes in the electronic configurations of the atoms or molecules. Unlike conduction and convection, the transfer of heat by radiation does not require the presence of an intervening medium.

There are two components of thermal radiation long-wave radiation and short-wave radiation.

The Stefan-Boltzmann law as describes long-wave energy emitted by all real surfaces

$$\dot{Q}_{emit} = \dot{Q}_{rad} = \varepsilon\sigma A_s T_s^4 \qquad (3.2.1.3.1)$$

Where:

- $\sigma=5.67\cdot10{-}8$ W/m². K⁴ is the Stefan-Boltzmann constant
- ε surface is surface emissivity (0–1)

Ts is the absolute surface temperature (K)

$\dot{Q}_{rad}$ is the radiative heat transfer rate (W)

[1] v (m/sec) denotes the wind speed adjacent to the surface.

Source of the long-wave radiation in our case are:

(1) Radiated heat exchanged by external walls

(2) Radiated heat exchange among internal surfaces of the walls

(3) Radiated heat exchange between occupants and internal surface of the walls

(4) Radiated heat exchange between lighting, office and lab equipment and internal wall surfaces

Direct use of the nonlinear Stefan–Boltzmann formulation for radiative heat transfer, i.e., $\dot{Q}_{emit}$ in the thermal model equations would violate the linearity assumptions required for state-space representation and MPC design. Therefore, approximate linearized formulations are adopted by defining an effective radiative heat transfer coefficient h_r, which is obtained through linearization of the Stefan–Boltzmann law around a nominal surface temperature.

This approach allows radiative heat transfer to be expressed in a linear form compatible with the state-space representation required for Model Predictive Control (MPC).

Specifically, effective linearized radiative heat transfer coefficients provided by ASHRAE and ISO 6946 standards are employed, depending on the source and characteristics of the radiative exchange.

For conductive building surfaces, radiative heat transfer effects are incorporated through the use of a combined surface heat transfer coefficient, defined as h=hc+hr, where hc represents the convective heat transfer coefficient and hr (**Table 3-2**)denotes the linearized radiative heat transfer coefficient (Çengel, 2020).

This combined coefficient is applied to all surfaces exposed to air, including the exterior surfaces of external walls as well as the interior surfaces of walls, ceilings, and floors in contact with indoor air. In the context of the present model, this formulation is applied to radiative sources (1) and (2) described above.

Table 3-2 Radiative Heat Transfer Coefficient

radiative coefficient; internal surface	4,59 (W/(m^2.K))
radiative coefficient; external surface	5,13 (W/(m^2.K))

For radiative sources (3) and (4), the relevant tables provided in the Internal Heat Gains section (Chapter 18) of (ASHRAE, 2017) are employed. The radiative heat emitted by these internal sources is aggregated and applied to the internal mass temperature node, Tm, within the thermal model, as described in a subsequent section.

Short-wave radiation generated by solar irradiation, which is addressed in a separate section below, is treated independently.

3.2.2 Thermal Load Components

3.2.2.1 Latent Heat Loads

The latent heat transfer rate (Q_{latent}) represents the hidden energy transfer rate associated with moisture changes in the air due to phase transitions such as evaporation or condensation. It can be expressed as:

$$\dot{Q}_{latent} = h_{fg}\, m_{dryair} \frac{dw}{dt} \qquad (3.2.2.1.1)$$

The latent heat can originate from multiple sources, including:

- HVAC system: Active moisture addition or removal (Q_{latent_hvac})
- Internal sources: Occupants' respiration, sweating, or equipment (Q_{latent_int})
- Infiltration: Moisture carried by air infiltration (Q_{latent_inf})
- Ventilation: Moisture carried by ventilation air (Q_{latent_vent})

The net latent heat transfer can therefore be formulated as:

$$Q_{latent\_net} = Q_{latent\_hvac} + Q_{latent\_int} + Q_{latent\_inf} + Q_{latent\_vent}$$

$$\frac{dw}{dt} = \frac{1}{h_{fg} m_{dryair}} \left(\dot{Q}_{latent\_hvac} + \dot{Q}_{latent\_int} + \dot{Q}_{latent\_inf} + \dot{Q}_{latent\_vent} \right)$$

The infiltration and ventilation contributions are given by:

$$\dot{Q}_{latent\_inf} = \dot{m}_{inf} h_{fg} \left(\omega_{fact} - \omega_{in} \right)$$

$$\dot{Q}_{latent\_vent} = \dot{m}_{vent} h_{fg} (\omega_{out} - \omega_{in})$$

Accordingly, the governing latent humidity equation can be written as

$$\frac{d\omega}{dt} = \frac{1}{m_{dry\_air} h_{fg}} [Q_{latent\_hvac} + Q_{latent\_int} + \dot{m}_{inf} h_{fg}(\omega_{fact} - \omega_{in}) + \dot{m}_{vent} h_{fg}(\omega_{out} - \omega_{in})$$

Where:

h_{fg} is specific enthalpy of vaporization constant. (J/kg_{water})

- The amount of energy required to convert a unit mass of liquid water into vapour (or released when vapour condenses) at a constant temperature. This value determines the energetic cost of adding or removing moisture.
- $m_{dry\_air\ is}$ mass of dry air in the subject volume (kg)
- dω/dt is the rate of change of humidity ration (kgwater(kgdry_air/sec))
- $\dot{m}_{inf}$ is infiltration air mass flow rate (kgdryair/sec)
- $\dot{m}_{vent}$ is ventilation air mass flow rate (kgdryair/sec)
- $\omega_{in}, \omega_{out}, \omega_{fact}$ are indoor, outdoor and factory humidity factors.

3.2.2.2 Sensible Heat Load

3.2.2.2.1 Internal Sensible Heat Loads

Internal heat gains represent the cumulative sensible heat generated within the system by occupants, electrical devices, lighting, and equipment. Depending on their thermal effect on the conditioned space, these contributions may be treated as positive (heat gains) or negative (effective heat losses) in the energy balance formulation.

The sensible portion of internal heat gains can be further decomposed into convective and radiative components. The convective component directly affects the indoor air temperature, whereas the radiative component is first absorbed by surrounding surfaces and internal masses before influencing the air temperature indirectly through subsequent heat exchange mechanisms.

3.2.2.2.2 HVAC Sensible Heat

This term represents the cumulative sensible heat introduced into or removed from the modeled space by active heating and cooling systems. In the present study, this contribution is provided exclusively by the HVAC system and constitutes a controlled

input within the energy balance formulation.

3.2.2.3 Solar Heat Load

Solar effects occur on exterior surfaces of the subject space envelops. Solar radiation contributes to heat gain in three primary mechanisms:
(1) Absorption of short-wave radiation by exterior wall surfaces,
(2) Transmission of solar radiation through glazing into the interior space, and
(3) long-wave radiative exchange.
The contribution of long-wave solar radiation is neglected in the present study, since the long-wave component of solar radiation is largely absorbed by the atmosphere and its direct impact on the building thermal energy balance is therefore negligible.

3.2.2.3.1 Solar Radiation Absorbed by Exterior Wall Surface

This is the portion of incident solar radiation on the exterior wall surface that is absorbed by the surface and transferred as heat into the wall. This absorbed energy increases the exterior surface temperature of the wall.

$$\dot{Q}_{solar\_wall} = A_{wall} \cdot \alpha_{solar} \cdot Q_{incident}$$

Where:

- $\dot{Q}_{solar\_wall}$ is the absorbed solar heat by the wall (W)
- A_{wall} is the exterior wall surface area exposed to solar radiation (m^2)
- α_{solar} is solar absorbance of the wall surface
- $Q_{incident}$ is total solar irradiance on the wall surface (W/m^2)

3.2.2.3.2 Solar Radiation Transmitted Through Window Surfaces

A significant portion of the solar heat gain enters the space through glazing surfaces and is converted into sensible heat within the conditioned space.

$$\dot{Q}_{solar\_window} = A_{window} \cdot SHGC \cdot Q_{incident}$$

Where:

- $\dot{Q}_{solar\_window}$ is solar heat gain transmitted through the window (W)

- A_{wall} is window surface area exposed to solar radiation (m^2)
- *SHGC (Solar Heat Gain Coefficient)* is a factor representing how much of the incident solar radiation is transmitted through the glass assembly into the interior space.
- $Q_{incident}$ is total solar irradiance on the window surface (W/m^2)

3.3 Lumped-Parameter Model

3.3.1 2R1C Envelope Modelling

3.3.1.1 Walls

The walls including floor and ceiling of the lab is like in **Figure 3.1**. External and internal layer are for higher insulations.

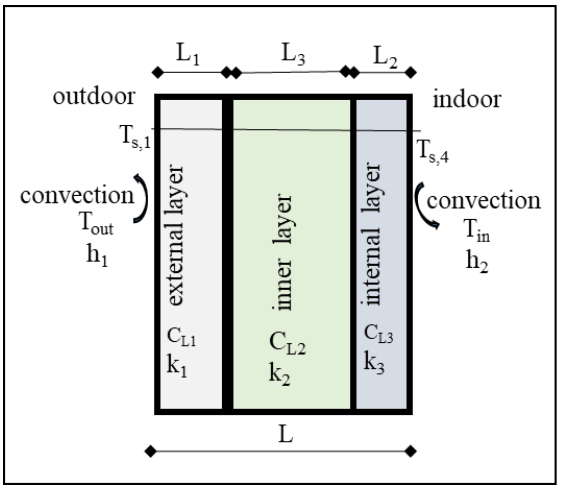

Figure 3-1 Wall Structure and Heat Transfer Mechanisms

There are 2R1C, 3R2C and 4R3C model approaches for envelope (wall) RC modelling[2]. Higher C models mean higher degree differential equations that requires non-linear analysis. Therefore, lumped 2R1C model is selected for the project.
RC thermal model of the wall is given below.

[2] Building Thermal-Network Models: A Comparative Analysis, Recommendations, and Perpectives

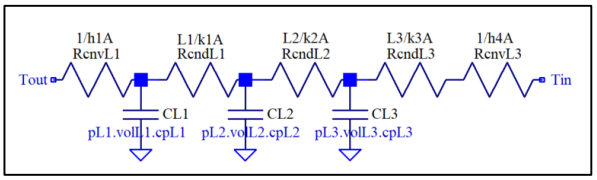

Where:

- R_{cnvL1}: Convection transfer between outside environment and surface of the L1 layer.
- R_{condL1}: Conduction transfer inside the L1 layer
- R_{condL2}: Conduction transfer inside the L2 layer
- R_{condL3}: Conduction transfer inside the L3 layer
- R_{cnvL}: Convection transfer between outer surface of the L2 layer and Internal environment
- C_{L1}, CL_2, CL_3: L1, L2 and L3 layer thermal capacitances /J/K)
- $p_{Li:}$ Density of the material of L1, L2 and L3 respectively (kg/m^3).
- $Vol_{Li:}$ Total volume of L1, L2 and L3 (m^3)
- cp_{Li}: Specific heat capacity of L1,L2 and L3 (J/(kg.K))

The lumped 2R1C model of above given model is

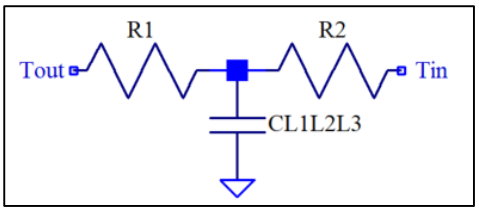

Where:

$$R_2 = R_1 = \frac{R_{total}}{2}$$

There are different methodologies available in the literature for determining the R1and R2parameters in 2R1C thermal modelling of building envelope elements (Tayler & Tarek), (Boodi, On Energy-Efficient Buildings Hybrd Dynamic Modelling for Analysis and Control, 2022).

In this study, the methodology proposed by (Tayler & Tarek) has been adopted due to its simplicity, transparency, and direct reliance on physical steady-state properties of the

building envelope. It should be noted that alternative methodologies for the calculation of R1 and R2 could be readily integrated into the proposed simulation framework.

$$C_{L1L2L2} = C_{L1} + C_{L2} + C_{L3}$$

$$R_{total} = R_{cnvL1} + R_{cndL1} + R_{cndL2} + R_{cndL3} + R_{cnvL3} \quad (3.1)$$

3.3.1.2 Windows and Door

Windows and doors are modelled as single-resistance (1R) elements, where heat transfer is represented solely by conduction through the component.

3.3.1.3 Internal Mass

The internal mass node represents only the thermal mass of indoor contents (furniture), while interior walls are modeled as separate nodes. The furniture is modeled using a 1R1C structure, and the total radiative component of internal heat gains is applied directly to this node.

Different approaches can be employed to estimate the thermal capacitance of internal contents:

(1) Physical method:

If sufficient information is available regarding the mass and material properties of the equipment and furniture used in the laboratory, the thermal capacitance can be calculated as:

$$C_m = \sum_i m_i . c_{p,i}$$

Where m_i is the mass of the i-th item and $c_{p,i}$ is its specific heat capacity.

(2) Equivalent internal capacitance without a separate indoor content node method:

In models where indoor contents are not represented by a dedicated thermal node, the effective internal thermal capacitance may be expressed by scaling the air capacitance with factor:

$$C_{in\_effective} = \alpha . C_{in} \quad (C_{in} = \rho_{air} . C_{\ pair} . V_{lab})$$

Where Cin denotes the thermal capacitance of the zone air only.

(3) Application of Method (2) with a separate internal mass node method when the indoor contents (furniture) are modeled as a separate thermal node Tm, the equivalent internal capacitance formulation in Method (2) can be adapted as:

$C_m = (\alpha - 1).C_{in}$

(4) (ISO 5. , 2017) based approach:

According to ISO 52016-1:2017 (Clause 6.5.11), the effective thermal capacitance of air and indoor contents is defined as 10 000 J/(m²·K). Based on this recommendation, the thermal capacitance of the internal mass node can be expressed as:

$C_m = 10000A_{floor} - C_{in}$

Where A_{floor} denotes the floor area of the laboratory.

In the simulation, ISO approach is used.

As for the Rm, It is calculated as $R_m = \frac{1}{hc+hr}\gamma A_{floor}$ where ϒ is is a scaling coefficient used to estimate the effective heat exchange area of furniture as a fraction of the floor area.

3.3.2 Aggregated RC Network Model

The laboratory is modeled as a single thermal zone. Under this assumption, thermal equilibrium within the space is assumed, and the indoor air temperature is considered spatially uniform. Accordingly, the air node is represented by a single thermal capacitance, denoted as C_{in}.

In the (Boodi, Beddiar, Amirat, & Benbouzid, 2022) it is stated that thermal-network models are predominantly applied to buildings by considering only sensible heat transfer dynamics, while latent heat effects are often completely neglected. This observation is valid for PhD thesis of Abhinandana Boodi (Boodi, On Energy-Efficient Buildings Hybrd Dynamic Modelling for Analysis and Control, 2022) as well.

The IEBB THEMA 2 Activity 4 Task 4.2 report (Taufiqoh, 2024) attributed the inconsistency observed between simulation results and measurements to unaccounted factor such as ventilation and infiltration, solar radiation, adjacent room interaction and possibly furniture thermal mass. It is also concluded there that a single zone RC model configuration not accounting for ventilation cannot be utilized.

The aggregated model (**Figure 3.2**) is constructed to include these components as comprehensively as possible within the adopted modelling framework.

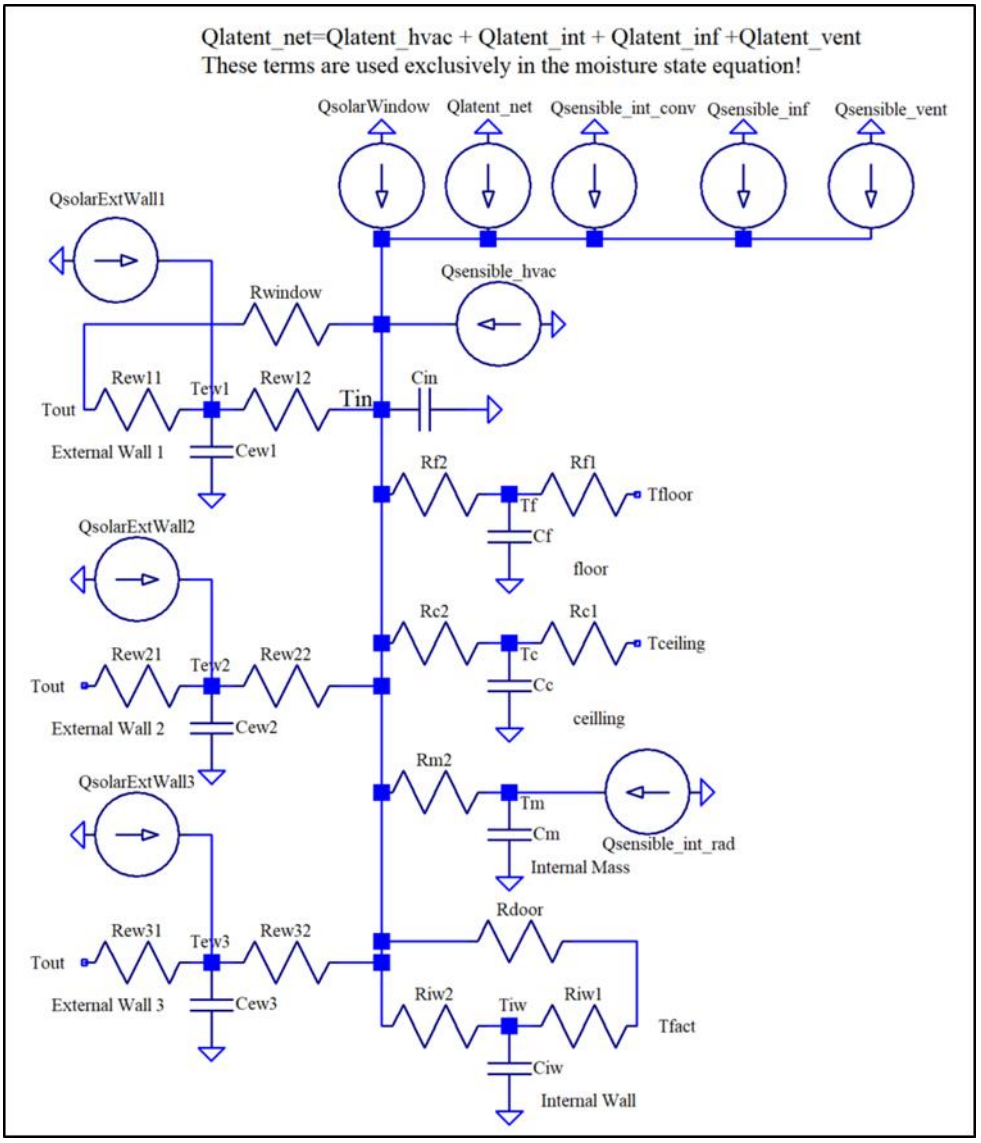

Figure 3-2 Aggregate Thermal Model of the Case Study Building

3.4 Differential Equations for Thermal and Moisture Dynamics

The differential equations describing the thermal and moisture behavior of the system are formulated based on the aggregated thermal model.

A consistent sign convention is adopted in the thermal and humidity dynamic formulations. Heat sources are defined as positive contributions, representing processes that increase the indoor air temperature of the laboratory. Conversely, heat sinks are defined as negative

contributions, representing mechanisms that extract thermal energy from the space and reduce the laboratory air temperature.

Thermal equation at nodes:

3.4.1 Node T_{in}

$$C_{in}\frac{dT_{in}}{dt} = \frac{T_{ew1}-T_{in}}{R_{ew12}} + \frac{T_{out}-T_{in}}{R_{window}} + \frac{T_{ew2}-T_{in}}{R_{ew22}} + \frac{T_{ew3}-T_{in}}{R_{ew32}} + \frac{T_{iw}-T_{in}}{R_{iw2}} + (1-\sigma)\frac{T_{fact}-T_{in}}{R_{door}} + \frac{T_m-T_{in}}{R_{m2}} + \frac{T_c-T_{in}}{R_{c2}} + \frac{T_f-T_{in}}{R_{f2}} + Q_{solarWin} + Q_{sensible_{hvac}} + Q_{sensiable_{int_{conv}}} + \sigma\, Q_{sensible\_inf} + Q_{sensible\_vent}$$

$Q_{sensible\_inf} = \dot{m}_{inf} c_p (T_{fact} - T_{in})$

$$C_{in}\frac{dT_{in}}{dt} = \frac{T_{ew1}-T_{in}}{R_{ew12}} + \frac{T_{out}-T_{in}}{R_{window}} + \frac{T_{ew2}-T_{in}}{R_{ew22}} + \frac{T_{ew3}-T_{in}}{R_{ew32}} + \frac{T_{iw}-T_{in}}{R_{iw2}} + (1-\sigma)\frac{T_{fact}-T_{in}}{R_{door}} + \frac{T_m-T_{in}}{R_{m2}} + \frac{T_c-T_{in}}{R_{c2}} + \frac{T_f-T_{in}}{R_{f2}} + Q_{solarWin} + Q_{sensible_{hvac}} + Q_{sensiable_{int_{conv}}} + \sigma\dot{m}_{inf} c_p (T_{fact} - T_{in}) + \dot{m}_{vent} c_p (T_{vent} - T_{in})$$

σ(t) is a time-averaged door opening factor representing the fraction of time within each simulation interval during which the door remains open. A value of σ=0 corresponds to a fully closed door, while σ=1represents a door that remains open for the entire interval. Intermediate values account for partial opening durations and enable simultaneous modulation of conductive and air-exchange heat transfer mechanisms.

3.4.2 Node T_{ew1}

$$C_{ew1}\frac{dT_{ew1}}{dt} = \frac{T_{out}-T_{ew}1}{R_{ew11}} + \frac{T_{in}-T_{ew1}}{R_{ew12}} + Q_{solarExWall1}$$

3.4.3 Node T_{ew2}

$$C_{ew2}\frac{dT_{ew2}}{dt} = \frac{T_{out}-T_{ew2}}{R_{ew21}} + \frac{T_{in}-T_{ew2}}{R_{ew22}} + Q_{solarExWall2}$$

3.4.4 Node T_{ew3}

$$C_{ew3}\frac{dT_{ew3}}{dt} = \frac{T_{out} - T_{ew3}}{R_{ew31}} + \frac{T_{in} - T_{ew3}}{R_{ew32}} + Q_{solarExWall3}$$

3.4.5 Node T_{iw}

$$C_{iw}\frac{dT_{iw}}{dt} = \frac{T_{fact} - T_{iw}}{R_{iw1}} + \frac{T_{in} - T_{iw}}{R_{iw2}}$$

3.4.6 Node T_f

$$C_f\frac{dT_f}{dt} = \frac{T_{floor} - T_f}{R_{f1}} + \frac{T_{in} - T_f}{R_{f2}}$$

3.4.7 Node T_c

$$C_c\frac{dT_c}{dt} = \frac{T_{ceiling} - T_c}{R_{c1}} + \frac{T_{in} - T_c}{R_{c2}}$$

3.4.8 Node T_m

$$C_m\frac{dT_m}{dt} = \frac{T_{in} - T_m}{R_{m2}} + Q_{sensible\_int\_rad}$$

3.4.9 Node Moisture

The following formula is used in our case.

$$\frac{d\omega}{dt} = \frac{1}{m_{dry\_air}h_{fg}}\left[Q_{latent\_hvac} + Q_{latent\_int} + \dot{m}_{inf}h_{fg}\sigma\left(\omega_{fact} - \omega_{in}\right) + \dot{m}_{vent}h_{fg}(\omega_{out} - \omega_{in})\right]$$

3.5 State-Space Representation of the Thermal Model

The thermal and humidity dynamics of the laboratory building, which is modelled, using the lumped Resistance-Capacitance (RC) network, are most effectively represented using the continuous-time state-space formulation. This linear, time-invariant (LTI) structure is the mathematical core of the Model Predictive Control (MPC) algorithm.

The dynamics of the system are governed by a set of coupled ordinary differential equations presented previous section are consolidated into the standard state-space form:

$$\dot{x}(t) = Ax(t) + Bu(t) + Dw(t)$$

$$y(t) = Cx(t) \quad (E=F=0)$$

In the present model, the output variables represent physical state quantities such as indoor air temperature and humidity ratio. These outputs are not directly influenced by the control or disturbance inputs, but rather evolve through the system dynamics captured by the state variables. Therefore, direct feedthrough terms are not considered, and the matrices E and F are set to zero.

Definition of State Space Variables:

State Vector Derivative, $\dot{\boldsymbol{x}}(\boldsymbol{t})$: Represent the rate of change of all system states.

State Vector, x(t): Includes all relevant thermal states and the indoor specific humidity. It appears on the left-hand side of the state equations. In this study, the state vector is defined as:

$x(t) = [T_{in}, Tew_1, Tew_2, T_{ew3}, T_{iw}, T_f, T_c, T_m, \omega_{in}]^T$

Control Input Vector, u (t): Represents the control actions applied exclusively by the HVAC system. These inputs correspond to the actively manipulated variables used by the controller to regulate indoor thermal comfort and humidity conditions. In this study, the control input vector is defined as:

$u(t) = [Q_{sensible\_hvac}, Q_{latent\_hvac}]^T$

Disturbance (Load) Vector, w(t): Represents external and internal thermal and moisture-related disturbances acting on the system. In this study, the disturbance vector is defined as:

$w(t) = [T_{out}, T_{fact}, T_{floor}, T_{ceiling}, Q_{solarWin}, Q_{solarExWall1}, Q_{solarExWall2}, Q_{solarExWall3}, Q_{sensible\_int\_conv}, Q_{sensible\_int\_rad}, \dot{m}_{inf}, Q_{latent\_int}, \omega_{fact}]^T$

Output Vector, y(t): Contains the measured and controlled variables of the system, namely the indoor air temperature and the indoor specific humidity ratio:

$y = [T_{in}, \omega_{in}]^T$

System Matrices:

A - System Dynamics Matrix: Defines the internal dynamics, calculated from all R and C values.

B - Control Input Matrix: Maps the HVAC control inputs (u) to the state derivatives ($\dot{x}$)

D - Disturbance Matrix: Maps the external and internal loads (w) to the state derivatives

C - Output Matrix: Selects the controlled variables from the state vector (x).

4 MODEL PREDICTIVE CONTROL (MPC) DESIGN

4.1 MPC Formulation and Control Objectives

This section sets the stage by formally defining the components of the linear time-invariant (LTI) state-space model that the MPC controller will use for prediction.

4.1.1 Control Objectives

The primary control objectives for the laboratory building are:

(1) Thermal Comfort Maintenance: Regulate the Indoor Air Temperature (Tin) to a predefined set point (T_{ref}) within configurable narrow comfort bounds.

(2) Humidity Control: Regulate the Indoor Specific Humidity (ω) to prevent condensation and maintain optimal air quality/comfort.

(3) Energy Efficiency: Minimize the overall control effort of the HVAC system by reducing the magnitude and variation of the control input vector u(t), while maintaining thermal and humidity comfort requirements.

(4) Configurability: Enable key model and control parameters to be configurable in order to evaluate their influence on system behavior and control performance. This configurability is intended to support sensitivity analysis and to allow the developed simulation framework to be used as an *educational and learning-oriented tool*.

4.2 Cost Function Definition

4.2.1 Structure of the Cost Function

The Cost Function serves two main purposes for optimization:

(1) Tracking and Comfort: To penalize deviations of the controlled outputs (y) from their target reference values (y_{ref}). This ensures that the primary objectives of maintaining indoor temperature (T_{in}) and specific humidity (ω) are met.

(2) Energy and Effort Minimization: To penalize excessive use of the control actuators (u). This prevents rapid cycling of the HVAC equipment and ensures the optimal, most energy-efficient control strategy is selected.

The formula:

$J=T_{tracking} + J_{efford} + J_{\Delta efford} + J_{slack}$

$$J = \sum_{i=1}^{N_p}\left(y_{k+1} - y_{ref}\right)^T Q\left(y_{k+1} - y_{ref}\right) + \sum_{i=0}^{N_c-1} u_{k+1}^T Ru_{k+1} +$$

$$\sum_{i=1}^{N_c-1} \Delta u_{k+1}^T S\Delta u_{k+1} + \sum_{1}^{N_p}(\varepsilon_i^{+T}\rho^+\varepsilon_i^+ + \varepsilon_i^{-T}\rho^-\varepsilon_i^-)$$

Where:

- $y= [T_{in}, \omega_{in}]^T$
- $u= [Q_{sens\_hvac}, Q_{latent\_hvac}]^T$
- $\Delta u_k = u_k - u_{k-1}$
- N_p Prediction horizon
- N_c: Control horizon
- $\sum_{1}^{N_p}(\varepsilon_i^{+T}\rho^+\varepsilon_i^+ + \varepsilon_i^{-T}\rho^-\varepsilon_i^-)$ (Soft constraint term)

Soft constraint term penalizes violations of output constraints through slack variables which are automatically determined by the MPC optimizer to preserve feasibility. The weighting matrices ρ^+ and ρ^-, defined by the user via the Error Cost Ratio (ECR), regulate the severity of constraint violations, enabling a controlled relaxation of constraints when necessary. $J_{tracking}$ minimizes the difference between predicted output (T_{in}, ω) and the desired reference or set point (y_{ref}). This the term responsible for comfort and set point adherence.

J_{efford} minimizes the magnitude of the control inputs (Q_{sens_hvac}, Q_{latent_hvac}). This is the primary term for energy efficiency and cost optimization. $J_{\Delta effort}$ minimizes the rate of change in the control inputs between consecutive time steps to ensure smooth control and contributes improved equipment longevity.

The core objective of the developed Model Predictive Control (MPC) strategy is to perform predictive control. This approach prioritizes operational cost minimization

(through the J_{effort} term in the cost function) while ensuring strict adherence to occupant and process comfort requirements. These constraints are defined as

$T_{min} \leq T_{in} \leq T_{max}$ $\omega_{min} \leq \omega_{in} \leq \omega_{max}$

4.2.2 Output Weighting Matrix (Q)

The weighting matrix Q defines the relative importance of tracking accuracy for the controlled outputs. Since the output vector consists of the indoor air temperature and indoor specific humidity, the matrix Q is defined as a diagonal matrix weighting deviations in Tin and ωin from their reference values.

Q=diag (qT, qW)

A higher weight is assigned to the indoor temperature to prioritize thermal comfort, while humidity regulation is enforced with a comparatively lower weight.

4.2.3 Input Weighting Matrix (R)

The matrix R penalizes the magnitude of the control inputs and represents the energy consumption of the HVAC system. Separate weights are assigned to the sensible and latent control inputs to reflect their different energetic and operational costs.

$R = diag(r_{sens}, r_{latent})$

Latent control is weighted more heavily due to the higher energy cost associated with dehumidification processes.

4.2.4 Input Rate Weighting Matrix (S)

The matrix S is included in the cost function formulation to represent penalties on the rate of change of control inputs. However, in the present study, S is set to a zero matrix, effectively disabling the input rate penalty. This choice is made to focus the controller behaviour on tracking performance and energy efficiency, while preserving the general MPC structure for future extensions.

$S = diag(0,0)$

4.2.5 Q and R Matrices Tuning

The weighting matrices Q and R are tuned using a structured, simulation-based approach. Initially, both matrices are normalized to account for differences in physical units and

magnitudes between the controlled outputs and control inputs.
For the output-weighting matrix Q, normalization is performed based on the allowable comfort deviations of indoor temperature and humidity.
For the input-weighting matrix R, normalization is performed based on the nominal maximum capacities of the HVAC actuators.
After normalization, priority factors are introduced to reflect control objectives, such as emphasizing thermal comfort over humidity regulation and penalizing latent HVAC power more heavily due to its higher energy cost. The resulting weighting coefficients are then validated through closed-loop MPC simulations under representative operating conditions.
The final values are selected to achieve a balanced trade-off between tracking performance, energy efficiency, and constraint satisfaction, while avoiding overly aggressive control actions.

Table 4-1 Q and R Configurable Parameters

Parameter	Definition	Value (Initial)	Unit	Description
Q Matrix				
Comfort factor	Temperature priority factor	1	-	Prioritization factor to enforce stricter temperature tracking. Configurable.
R Matrix				
Energy factor	Latent energy priority factor	1	-	Scaling factor reflecting the higher energy cost of latent control. Configurable.

4.3 System Constraints

4.3.1 X State Vector Constraint

Table 4-2 X State Vector Constraints

Constraint Type	Variable	Description	Mathematical Form
Indoor Temperature (Comfort)	T_{in}	Enforces the thermal comfort band required by the laboratory specifications. Configurable	$T_{in}^{min} \leq T_{in\_}(k+i) \leq_{Tin}^{max}$
Indoor Humidity (Comfort)	ω_{in}	Prevents condensation, mold growth, and ensures air quality necessary for processes and health. Configurable.	$\omega_{in}^{min} \leq \omega_{in}(k+i) \leq \omega_{in}^{max}$

Variable	Constraint Type	Value	Unit	Rationale
T_{in}	Lower Bound (T_{in_min})	22.0	◦C	Minimum acceptable cooling/heating set point.
T_{in}	Upper Bound (T_{in_max})	24.0	◦C	Maximum acceptable heating set point.
ω_{in}	Lower Bound (ω_{in_min})	0.007	kg_{water} /kg_{dry_air}	Approximately 40% Relative Humidity at 23◦C.
ω_{in}	Upper Bound (ω_{in_max})	0.012	kg_{water} /kg_{dry_air}	Approximately 65% Relative Humidity at 23◦C.

4.3.2 U Input Constraints

Table 4-3 U Input Constraints

Constraint Type	Variable	Description	Mathematical Form
HVAC Power (Sensible Load)	$Q_{sensible\_hvac}$	Limited by the maximum output of the cooler/heater unit. Configurable.	$Q_{sensible\_hvac}^{min} \leq Q_{sensible\_hvac}(k+i) \leq Q_{sensible\_hvac}^{max}$
Latent Power (Dehum/Hum)	Q_{latent_hvac}	Limited by the maximum power dedicated to moisture control. Configurable.	$Q_{latent\_hvac}^{min} \leq Q_{latent\_hvac}(k+i) \leq Q_{latent\_hvac}^{max}$

Variable	Constraint Type	Value	Unit	Rationale
$Q_{sensible\_hvac}$	Lower Bound $Q_{sensible\_hvac\_min}$	-5.000	W	Maximum capacity for sensible cooling (e.g., 5 kW cooling power).
$Q_{sensible\_hvac}$	Upper Bound $Q_{sensible\_hvac\_max}$	+5,000	W	Maximum capacity for sensible heating (e.g., 5 kW heating power).
Q_{latent_hvac}	Lower Bound $Q_{latent\_hvac\_min}$	-3.000	W	Maximum capacity for dehumidification (latent cooling).
Q_{latent_hvac}	Upper Bound $Q_{latent\_hvac\_max}$	+3,000	W	Maximum capacity for humidification (latent heating).

4.3.3 Other Required Model Constants

Table 4-4 Other Constraints

Constant	Description	Value	Unit
c_p	Specific Heat of Air	1006	J/(kg·K)
h_{fg}	Latent Heat of Vaporization	2,500,000	J/kgwater
m_{dry_air}	Mass of Dry Air in the Room	1200	kgkh

4.4 Discrete-Time Model for MPC

4.4.1 Continuous-Time State-Space Matrices (A, B, D and C)

$\dot{x}(t) = Ax(t) + Bu(t) + Dw(t)$

$x(t) = [T_{in}, T_{ew1}, T_{ew2}, T_{ew3}, T_{iw}, T_f, T_c, T_m, \omega_{in}]^T$

$u(t) = [Q_{sensible\_hvac}, Q_{latent\_hvac}]^T$

$w(t)=[T_{out},T_{fact},T_{floor},T_{ceiling},Q_{solarWin},Q_{solarExWall1},\ Q_{solarExWall2},\ Q_{solarExWall3},Q_{sensible\_int\_conv},$

$Q_{sensible\_int\_rad}, \dot{m}_{inf}, Q_{latent\_int}, \omega_{fact}, \dot{m}_{vent}, \omega_{out}]^T$

Given the state-space equation and the Matrices defined above the following formulation is used to identify the matrix elements.

$$\dot{x}_i(t) = \sum_{j=1}^{n} A_{ij}x_j(t) + \sum_{k=1}^{m} B_{ik}u_k(t) + \sum_{l=1}^{m} D_{il}w_l(t)$$

From this formulation:

- **i** denotes the i_{th} state (or node) dynamic equation. (T_{in} node is the first)
- **j** denotes the index of the j-th state variable in the state vector x. (T_{in} is the first element)
- **k** denotes the index of the k-th control input in input vector u. ($Q_{sensible\_hvac}$ is the first element)
- **l** denotes the index of the l-th disturbance input in disturbance vector w. (T_{out} is the first element)

4.4.1.1 Tin

$$C_{in}\frac{dT_{in}}{dt} = \frac{T_{ew1}-T_{in}}{R_{ew12}} + \frac{T_{out}-T_{in}}{R_{window}} + \frac{T_{ew2}-T_{in}}{R_{ew22}} + \frac{T_{ew3}-T_{in}}{R_{ew32}} + \frac{T_{iw}-T_{in}}{R_{iw2}} + (1-\sigma)\frac{T_{fact}-T_{in}}{R_{door}} + \frac{T_m-T_{in}}{R_{m2}} + \frac{T_c-T_{in}}{R_{c2}} + \frac{T_f-T_{in}}{R_{f2}} + Q_{solarWin} + Q_{sensible_{hvac}} + Q_{sensiable_{int_{conv}}} + \sigma\dot{m}_{inf}c_p\left(T_{fact}-T_{in}\right) + \dot{m}_{vent}c_p(T_{out}-T_{in})$$

Matrix A:

$A_{11} = -\frac{1}{C_{in}}\left(\frac{1}{R_{ew12}} + \frac{1}{R_{window}} + \frac{1}{R_{ew22}} + \frac{1}{w_{ew32}} + \frac{1}{R_{iw2}} + \frac{1-\sigma}{R_{door}} + \frac{1}{R_{m2}} + \frac{1}{R_{c2}} + \frac{1}{R_{f2}} + \sigma\dot{m}_{inf}c_p + \dot{m}_{vent}c_p\right)$ (T_{in})

$A_{12} = \frac{1}{C_{in}R_{ew12}}$ (T_{ew1})

$A_{13} = \frac{1}{C_{in}R_{ew22}}$ (T_{ew2})

$A_{14} = \frac{1}{C_{in}R_{ew32}}$ (T_{ew3})

$A_{15} = \frac{1}{C_{in}R_{iw2}}$ (T_{iw})

$A_{16} = \frac{1}{C_{in}R_{f2}}$ (T_f)

$A_{17} = \frac{1}{C_{in}R_{c2}}$ (T_c)

$A_{18} = \frac{1}{C_{in}R_{m2}}$ (T_m)

$A_{19} = 0$

Matrix B:

$B_{11} = \frac{1}{C_{in}}$ ($Q_{Sensible\_hvac}$)

$B_{12} = 0$ (Q_{latent_hvac})

Matrix D:

$D_{11} = \frac{1}{C_{in}R_{window}} + \frac{\dot{m}_{vent}c_p}{C_{in}}$ (T_{out})

$D_{12} = \frac{1}{C_{in}}(\frac{1-\sigma}{R_{door}} + \sigma\dot{m}_{inf}c_p)$ (T_{fact})

$D_{15} = \frac{1}{C_{in}}$ ($Q_{solarWin}$)

$D_{19} = \frac{1}{C_{in}}$ ($Q_{sens\_int\_conv}$)

$D_{13} = D_{14} = D_{16} = D_{17} = D_{18} = D_{110} = D_{111} = D_{112} = D_{113} = D_{114} = D_{115}0$

4.4.1.2 T_{ew1}

$C_{ew1}\frac{dT_{ew1}}{dt} = \frac{T_{out}-T_{ew}1}{R_{ew11}} + \frac{T_{in}-T_{ew1}}{R_{ew12}} + Q_{solarExWall1}$

Matrix A:

$A_{21} = \frac{1}{C_{ew1}R_{ew12}}$ (T_{in})

$A_{22} = -\left(\frac{1}{C_{ew1}R_{ew11}} + \frac{1}{C_{ew1}R_{ew12}}\right)$ (T_{ew1})

$A_{23} = A_{24} = A_{25} = A_{26} = A_{27} = A_{28} = A_{29} = 0$

Matrix B:

$B_{21} = 0$ ($Q_{Sensible\_hvac}$)

$B_{22} = 0$ (Q_{latent_hvac})

Matrix D:

$D_{21} = \frac{1}{C_{ew1}R_{ew11}}$ (T_{out})

$D_{26} = \frac{1}{C_{ew1}}$ ($T_{solarExWall1}$)

$D_{22} = D_{23} = D_{25} = D_{27} = D_{28} = D_{29} = D_{210} = D_{211} = D_{212} = D_{213} = D_{214} = D_{215} = 0$

4.4.1.3 Tew2

$C_{ew2}\frac{dT_{ew2}}{dt} = \frac{T_{out}-T_{ew2}}{R_{ew21}} + \frac{T_{in}-T_{ew2}}{R_{ew22}} + Q_{solarExWall2}$

Matrix A:

$A_{31} = \frac{1}{C_{ew2}R\_R_{ew22}}$ (T_{in})

$A_{33} = -(\frac{1}{C_{ew2}R_{ew21}} + \frac{1}{C_{ew2}R_{ew22}})$ (T_{ew2})

$A_{32} = A_{34} = A_{35} = A_{36} = A_{37} = A = 38 = A_{39} = 0$

Matrix B:

$B_{31} = B_{32} = 0$

Matrix D:

$D_{31} = \frac{1}{C_{ew2}R_{ew21}}$ (T_{out})

$D_{37} = \frac{1}{C_{ew2}}$ ($Q_{solarExWall2}$)

$D_{32} = D_{33} = D_{34} = D_{35} = D_{36} = D_{38} = D_{39} = D_{310} = D_{311} = D_{312} = D_{313} = D_{314} = D_{315} = 0$

4.4.1.4 Tew3

$$C_{ew3}\frac{dT_{ew3}}{dt} = \frac{T_{out} - T_{ew3}}{R_{ew31}} + \frac{T_{in} - T_{ew3}}{R_{ew32}} + Q_{solarExWall3}$$

Matrix A:

$A_{41} = \frac{1}{C_{ew3}R_{ew32}}$ (T_{in})

$A_{44} = -(\frac{1}{C_{ew3}R_{ew31}} + \frac{1}{C_{ew3}R_{ew32}})$ (T_{ew3})

$A_{42} = A_{43} = A_{45} = A_{46} = A_{47} = A_{48} = A_{49} = 0$

Matrix B:

$B_{41} = B_{42} = 0$

Matrix D:

$D_{41} = \frac{1}{C_{ew3}R_{ew31}}$ (T_{out})

$D_{48} = \frac{1}{C_{ew3}}$ ($Q_{solarExWall3}$)

$D_{42} = D_{43} = D_{44} = D_{45} = D_{46} = D_{47} = D_{49} = D_{410} = D_{411} = D_{412} = D_{413} = D_{414} = D_{415} = 0$

4.4.1.5 Tiw

$$C_{iw}\frac{dT_{iw}}{dt} = \frac{T_{fact} - T_{iw}}{R_{iw1}} + \frac{T_{in} - T_{iw}}{R_{iw2}}$$

Matrix A:

$A_{51} = \frac{1}{C_{iw}R_{iw2}}$ (T_{in})

$A_{55} = -(\frac{1}{C_{iw}R_{iw1}} + \frac{1}{C_{iw}R_{iw2}})$ (T_{iw})

$A_{52} = A_{53} = A_{54} = A_{56} = A_{57} = A_{58} = A_{59} = 0$

Matrix B:

$B_{51} = B_{52} = 0$

Matrix D:

$D_{52} = \frac{1}{C_{iw}R_{iw1}}$ (T_{fact})

$D_{51} = D_{53} = D_{54} = D_{55} = D_{56} = D_{47} = D_{58} = D_{59} = D_{510} = D_{511} = D_{512} = D_{513}$
$= D_{514} = D_{515} = 0$

4.4.1.6 Tf

$$C_f \frac{dT_f}{dt} = \frac{T_{floor} - T_f}{R_{f1}} + \frac{T_{in} - T_f}{R_{f2}}$$

Matrix A:

$A_{61} = \frac{1}{C_f R_{f2}}$ (T_{in})

$A_{66} = -(\frac{1}{C_f R_{f1}} + \frac{1}{C_f R_{f2}})$ (T_f)

$A_{62} = A_{63} = A_{64} = A_{65} = A_{67} = A_{68} = A_{69} = 0$

Matrix B:

$B_{61} = B_{62} = 0$

Matrix D:

$D_{63} = \frac{1}{C_f R_{f1}}$ (T_{floor})

$D_{61} = D_{62} = D_{64} = D_{65} = D_{66} = D_{67} = D_{68} = D_{69} = D_{610} = D_{611} = D_{612} = D_{613}$
$= D_{614} = D_{615} = 0$

4.4.1.7 Tc

$$C_c \frac{dT_c}{dt} = \frac{T_{ceiling} - T_c}{R_{c1}} + \frac{T_{in} - T_c}{R_{c2}}$$

Matrix A:

$A_{71} = \frac{1}{C_c R_{c2}}$ (T_{in})

$A_{77} = -(\frac{1}{C_c R_{c1}} + \frac{1}{C_c R_{c2}})$ (T_c)

$A_{72} = A_{73} = A_{74} = A_{75} = A_{76} = A_{78} = A_{79} = 0$

Matrix B:

$B_{71} = B_{72} = 0$

Matrix D:

$D_{74} = \frac{1}{C_c R_{c1}}$ ($T_{ceiling}$)

$D_{71} = D_{72} = D_{73} = D_{75} = D_{76} = D_{77} = D_{78} = D_{79} = D_{710} = D_{711} = D_{712} = D_{713} = D_{714} = D_{715} = 0$

4.4.1.8 Tm

$$C_m \frac{dT_m}{dt} = \frac{T_{in} - T_m}{R_{m2}} + Q_{sensible\_int\_rad}$$

Matrix A:

$A_{81} = \frac{1}{C_m R_{m2}}$ (T_{in})

$A_{88} = -(\frac{1}{C_m R_{m2}})$ (T_m)

$A_{82} = A_{83} = A_{84} = A_{85} = A_{86} = A_{87} = A_{89} = 0$

Matrix B:

$B_{81} = B_{82} = 0$

Matrix D:

$D_{810} = \frac{1}{C_m}$ ($Q_{sensible\_int\_rad}$)

$D_{81} = D_{82} = D_{83} = D_{84} = D_{85} = D_{86} = D_{87} = D_{88} = D_{89} = D_{811} = D_{812} = D_{813} = D_{814} = D_{815} = 0$

4.4.1.9 ωin

$$\frac{d\omega}{dt} = \frac{1}{m_{dry\_air} h_{fg}} [Q_{laten_{hvac}} + Q_{latent_{int}} + \sigma \dot{m}_{inf} h_{fg}(\omega_{fact} - \omega_{in}) + \dot{m}_{vent} h_{fg}(\omega_{out} - \omega_{in})]$$

Matrix A:

$A_{99} = -(\frac{\sigma \dot{m}_{inf}}{m_{dry_{air}}} + \frac{\dot{m}_{vent}}{m_{dry_{air}}})$ (ω_{in})

$A_{91} = A_{92} = A_{93} = A_{94} = A_{95} = A_{96} = A_{97} = A_{98} = 0$

Matrix B:

$B_{91} = 0$ ($Q_{Sensible\_hvac}$)

$B_{92} = \frac{1}{m_{dry\_air} h_{fg}}$ (Q_{latent_hvac})

Matrix D:

$D_{912} = \frac{1}{h_{fg} m_{dry\_air}} \quad (Q_{latent\_int})$

$D_{913} = \frac{\sigma \dot{m}_{inf}}{m_{dry\_air}}$

$D_{915} = \frac{\dot{m}_{vent}}{m_{dry\_air}}$

$D_{91} = D_{92} = \mathrm{D}_{93} = D_{94} = D_{95} = D_{96} = D_{97} = D_{98} = D_{99} = \mathrm{D}_{910} = \mathrm{D}_{911} = \mathrm{D}_{914} = 0$

4.4.1.10 Output Matrix y(t)

$Y = [T_{in}, \omega_{in}]^T = Cx$

$C_{11} = 1 \quad (T_{in})$

$C_{29} = 1 \quad (\omega_{in})$

$C_{12} = C_{13} = C_{14} = C_{15} = C_{16} = C_{17} = C_{18} = C_{19} = 0$

$C_{21} = C_{22} = C_{23} = C_{24} = C_{25} = C_{26} = C_{27} = C_{28} = 0$

4.5 Discrete-Time State-Space Matrices (A_d, B_d, D_d)

The continuous-time state-space model derived from the RC thermal–humidity network is converted into a discrete-time representation for use within the MPC framework.

A zero-order hold (ZOH) assumption is adopted, in which the control inputs and disturbance signals are assumed to remain constant over each sampling interval Ts.

Discrete-Tie Space Equation:

$x(k+1) = A_d x(k) + B_d u(k) + D_d w(k)$

$y(k) = C_d x(k)$

The discrete-time system Matrices (A_d, B_d, D_d) are obtained using MATLAB's built-in c2d function with the ZOH option, ensuring exact discretization of the continuous-time model for the selected sampling time Ts.

5 SIMULATION IMPLEMENTATION

5.1 Model Parameterization (Thermal Resistances and Capacitances)

Model parameterization, calculating resistance and capacitor is performed in *SimulationTable_3_1_2026.xls* with selected real physical building properties. MATLAB simulation reads the model parameters from this excel file.

In addition to the static envelope parameters, the thermal interaction associated with the laboratory door is modelled using a time-averaged approach. When the door is open, conductive heat transfer through the door leaf is neglected and heat transfer is assumed to occur solely via air exchange. Accordingly, the conductive heat transfer term associated with the door is weighted by (1−σ) (1-\sigma) (1−σ), representing the fraction of time within each simulation interval during which the door remains closed.

5.2 Winter Disturbance Scenarios

5.2.1 Winter Disturbance Scenario (Istanbul – January)

A winter disturbance scenario was developed to represent representative January morning in Istanbul. The scenario spans the period between 00:00 and 24:00 with a temporal resolution of one hour, allowing the MPC controller to capture gradual variations in environmental conditions. Most of the values are taken from weather archive in National Laboratory of the Rockies.

Details can be found in *SimulationTable_3_1_2026**.xls***. MATLAB simulation reads the disturbance terms from this excel file.

5.3 Ventilation and Infiltration Calculations

ASHRAE could not be used for the calculation since the relevant ASHRAE document are unavailable. Google search is used for this section.

5.3.1 Ventilation

The ventilation mass flow rate is calculated as:

$\dot{m}_{vent} = \rho_{dryair} \frac{ACH.V_{zone}}{3600}$ (Kg/sec)

Where:

- $\dot{m}_{vent}$ is ventilation mass flow rate as kg/sec
- ACH is air changes per hour (h^{-1})
- ρ_{dryair} is air density (assumed as. 1.2 kg/m^3)
- V_{zone} is volume of the zone (m^3)
- 3600 is number of the seconds in an hour

For the present study, the air change rate is assumed to be:

ACH=10.

Ventilation air is assumed outdoor air at Tout.

5.3.2 Infiltration

Infiltration during door-opening periods is calculated using the same formulation as mechanical ventilation, with a different air change rate (ACH).

For the present study, the air change rate is assumed to be:

ACH = 0,5

In the adopted modeling approach, infiltration is considered only during door-opening periods. Infiltration through walls, windows, and other unintended leakage paths is assumed negligible and therefore not included in the thermal model.

5.4 Implemented Cost Function

The cost function adopted in the simulation

$J_{total} = \Sigma\ (qT\ (Tin - Tref)^2 + qW\ (win - wref)^2) + \Sigma\ rSensQ_{senible\_hvac}^2 + rLatQ_{latent\_hvac}^2) + \Sigma(s\Delta u^2) + \Sigma(ECR\varepsilon^2)$,

Which can be decomposed as

$J_{total} = J_{comfort} + J_{control} + J_s + J_{slack}$

All summations are evaluated over the prediction horizon, which spans 24 hours.

Humans respond more rapidly and more directly to temperature variations than to changes in humidity. Consequently, thermal comfort is generally considered more critical than humidity comfort in building operation and control.

To reflect this distinction, the temperature tracking weight qT is explicitly scaled by a comfort factor, which allows the relative importance of thermal comfort to be adjusted independently. In contrast, the humidity tracking weight is not directly scaled by the

comfort factor, reflecting the assumption that short-term humidity deviations are tolerable.

Furthermore, the energetic cost of humidity control is governed by a separate parameter, the energy factor, which scales the penalty associated with the latent HVAC actuation. This design choice acknowledges that humidification and dehumidification processes are typically more energy-intensive and operationally costly than sensible heating or cooling. As a result, humidity regulation is penalized primarily through control effort rather than tracking accuracy.

In contrast, sensible temperature control is not directly affected by the energy factor, ensuring that thermal comfort remains the dominant objective even when energy penalties are increased. This asymmetric weighting strategy allows the MPC to enforce strict temperature regulation while treating humidity control as a secondary, economically moderated objective. Such a formulation is consistent with the intrinsic nature of thermal and moisture comfort, where temperature deviations cause immediate discomfort and rapid energy imbalance, whereas humidity deviations evolve more slowly and can be tolerated for limited periods, particularly during winter operation.

Both the comfort factor and the energy factor can be adjusted via the graphical user interface (GUI).

In the simulation, soft constraints are applied to the output variables in accordance with the recommendations of the MATLAB MPC Toolbox. Accordingly, the global slack penalty weight (Weights.ECR) is employed to penalize violations of the output constraints, thereby allowing limited constraint relaxation when strict enforcement would lead to a higher overall cost.

At each sampling instant, the MPC determines the optimal control action by comparing the total predicted cost of all feasible candidate control sequences over the entire prediction horizon, rather than evaluating only the immediate cost at the current time step. The control sequence that yields the minimum total cost is selected, and only its first control move is applied to the system. This predictive evaluation enables the controller to account for future system behavior and, when necessary, to take anticipatory control actions in order to minimize the overall cost.

5.5 Switched-LTI Modelling of Time-Varying Disturbances

Infiltration and ventilation effects are treated as disturbances whose magnitudes vary on an hourly basis, consistent with the selected sampling time of 60 minutes. As a result, the assumption of a strictly linear time-invariant (LTI) model is violated. To address this issue, a switched linear time-invariant (switched-LTI) modeling approach is employed, in which the system matrices are updated at each sampling interval. This approach enables the incorporation of time-varying disturbance effects while preserving the computational simplicity of LTI-based MPC formulations.

6 SIMULATION RESULTS AND DISCUSSION

6.1 Simulation Tests

6.1.1 Preparation Test

- **Action-1**: To obtain a baseline reference of the building dynamics without active HVAC intervention, the sensible and latent HVAC power limits are constrained to ±1 W over a 24-hour simulation horizon. All external disturbances and internal loads are applied as defined in the scenario. The MPC controller remains active but its influence on the system is negligible due to the imposed actuator constraints.

- **Observation-1**: Indoor temperature and humidity evolve solely under the influence of disturbances, revealing time intervals where comfort limits are violated. Although HVAC power remains near zero, the MPC control signals saturate at their bounds during these periods, indicating when and in which mode (sensible or latent) active control would be required. This experiment establishes an uncontrolled baseline against which subsequent HVAC-enabled simulations are evaluated (**Figure 6.1**).

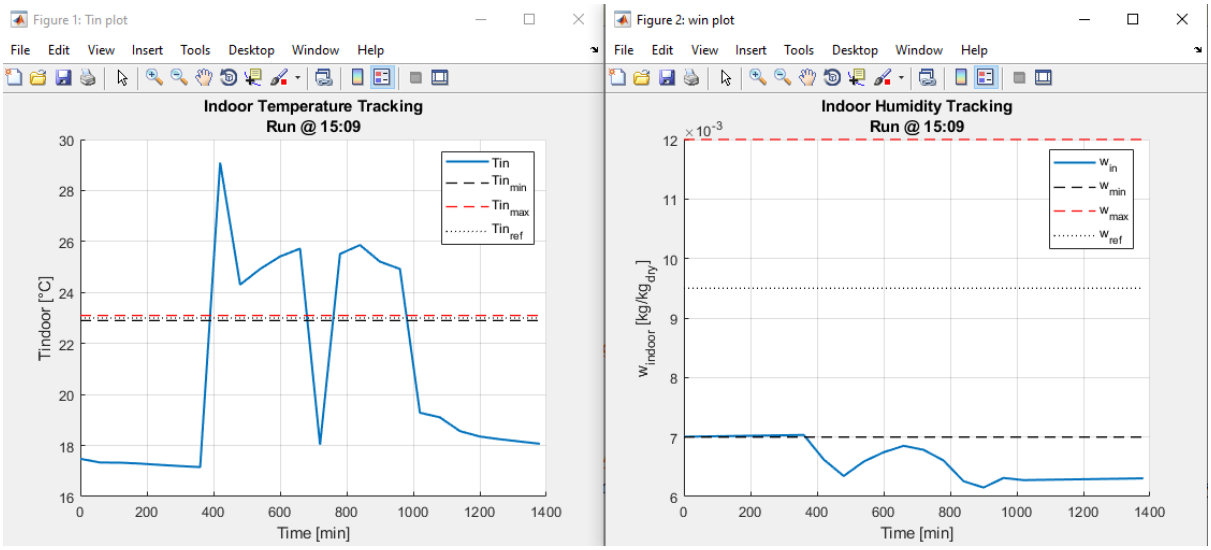

Figure 6-1 Temperature & Humidity Tracking Baseline Test

The initial conditions of the building thermal states were defined by assuming a fully thermally equilibrated building at 18 °C. This assumption represents a building that has been previously conditioned for an extended period prior to the start of the simulation. Consequently, when the HVAC system is disabled, the indoor air temperature remains close to the initial value throughout the 24-hour simulation horizon, despite lower outdoor temperatures. Modifying the initial temperature in the model directly shifts the starting point of the indoor temperature trajectory accordingly.

The same interpretation applies to the indoor humidity tracking results. The initial conditions of the indoor humidity states were defined by assuming a fully moisture-equilibrated indoor environment at the selected initial humidity ratio. Consequently, when latent HVAC control is disabled, the indoor humidity ratio remains close to its initial value over the 24-hour simulation horizon, despite variations in outdoor humidity conditions. Changing the initial indoor humidity value therefore shifts the initial point of the humidity trajectory accordingly.

6.2 Temperature Tracking Tests

6.2.1 Insufficient HVAC Power

- **Action-1:** The simulation is executed using the default parameter values specified through the graphical user interface (GUI).

- **Observation-1**: A noticeable drop in the indoor temperature (Tin) is observed during lunch period, between 12:00 and 13:00. This temperature decrease is primarily caused by a reduction in thermal sensible heat gains, Qsensibe_int_conv and Qsensible_int_rad components as confirmed by the corresponding disturbance plots or relevant MPC_Result_Run_at_hhmm excel file.

  Although the Model Predictive Controller attempts to compensate for this thermal deficit, the HVAC sensible heat input (Qsensible_hvac) reaches its upper operational limit and is therefore unable to fully offset the loss, resulting in a temporary thermal comfort violation (**Figure 6.2**). The sensible HVAC input is positive, as it represents heating supplied to the indoor space.

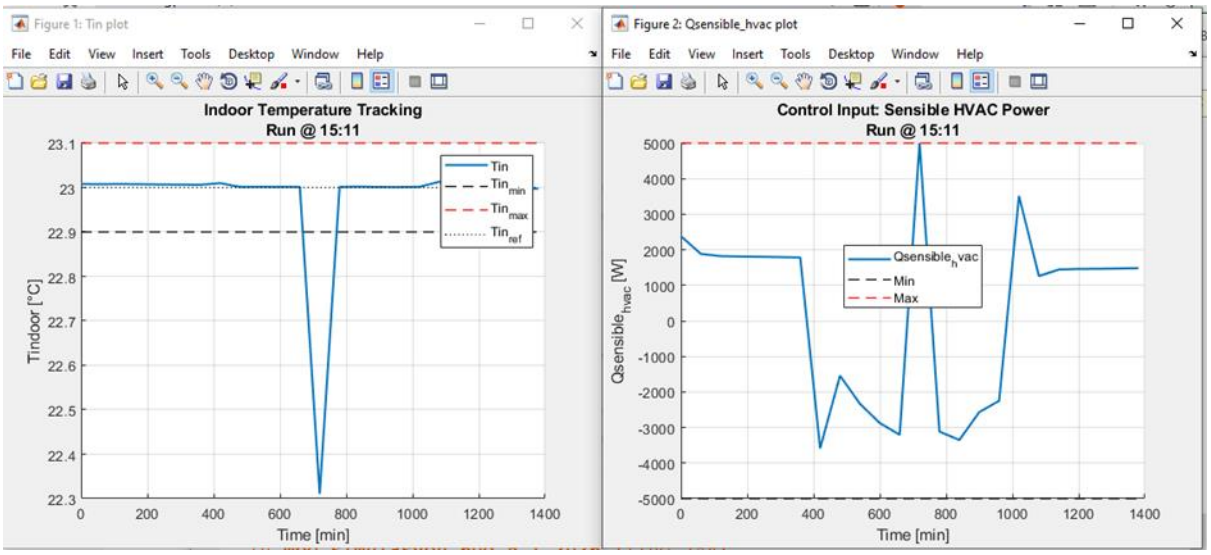

Figure 6-2 Temperature Tracking-Insufficient HVAC Power[3]

- **WARNING**: This test is expected to fail if Constraint_Type = 0 (hard constraint). Hard constraints may prevent the MPC from finding a feasible solution under the given scenario. Refer to the "Overly Stringent Constraints" test case for more details.
- **Note**: This test demonstrates that using soft constraints—even when the allowable margin is narrow—enables the MPC to successfully compute feasible control actions.

[3] The time axis is arranged to represent a 24-hour period according to the applied scenario.

6.2.2 Sufficient HVAC Power

- **Action-1**: The simulation is repeated after increasing the HVAC sensible heating capacity to *Qsensible_hvac = 6000 W* via the GUI in order to evaluate whether the increased heating capacity can compensate for the observed thermal discomfort.
- **Observation-1:** The indoor temperature drop is successfully compensated, and *Tin* remains within the predefined comfort range throughout the entire simulation period. This result confirms that the previously observed thermal comfort violation was caused by insufficient HVAC sensible heating capacity rather than limitations in the MPC formulation or tuning parameters, thereby demonstrating the adequacy of the controller when sufficient HVAC power is available (**Figure 6.3**).

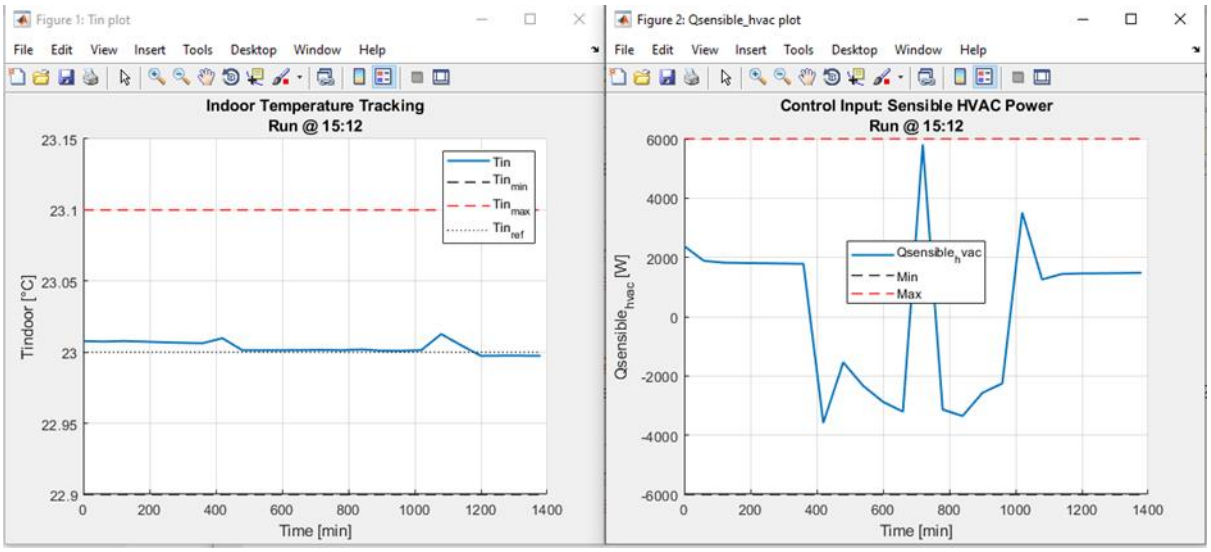

Figure 6-3 Temperature Tracking - Sufficient HVAC Power

Figure 6.2.2.1

6.2.3 Impact of the Cost Function on Temperature Tracking Test

- **Action-1** (***comfort cost test***) : The simulation is repeated after increasing the HVAC sensible heating capacity to *Qsensible_hvac = 6000 W, slew_rate_factor=0, and comfort_factor = 0.*01 via the GUI. The comfort factor is intentionally decreased. Increasing this parameter would not affect the results,

since perfect tracking has already been achieved under the given operating conditions.

The expectation is that the controller would relax temperature-tracking performance, allowing larger deviations from the reference and constraint bounds, since comfort violations become comparatively inexpensive with respect to control effort.

- **Observation-1**: The indoor temperature tracking and sensible HVAC power profiles remain largely similar to those obtained in the "Sufficient HVAC Power" temperature tracking test. However, a noticeable deviation from the temperature reference Tin_ref is observed, indicating that adherence to the temperature constraint is relaxed when the temperature tracking penalty is significantly reduced (**Figure 6.4**).

  Although the comfort factor was reduced, no substantial decrease in the HVAC power magnitude was observed. This indicates that relaxing the output tracking penalty alone does not necessarily lead to lower control effort, unless the input weighting (R matrix) associated with the corresponding manipulated variable is explicitly increased. In the adopted cost function formulation, the sensible HVAC power is not directly penalized through the energy_factor parameter; therefore, its usage cannot be effectively reduced via energy_factor tuning. As a result, the MPC maintains a similar actuation level while allowing larger temperature deviations.

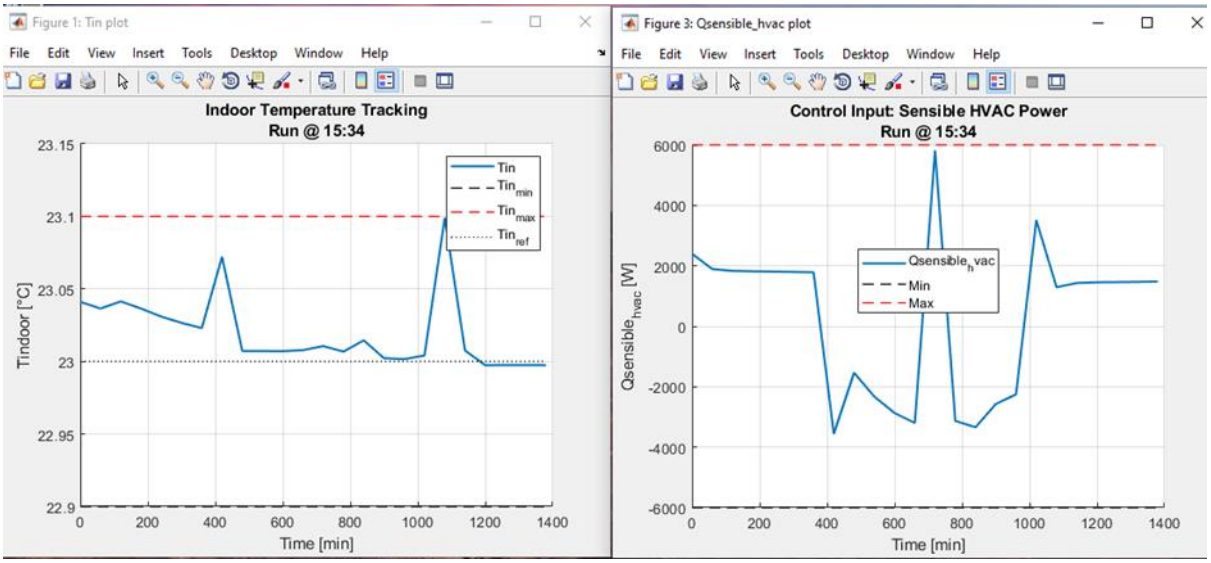

Figure 6-4 Impact of the Cost Function on Temperature Tracking

- **Action-2** (***control cost test***): The simulation is executed using the default parameter values specified except that the energy factor is increased to Energy_Factor = 10 via the graphical user interface (GUI).
- **Observation-2**: No noticeable change in system behavior is observed. Increasing the energy factor further, up to Energy_Factor = 1000 does not result in any observable difference in the control action or output trajectories.

  This behavior may be attributed to the relatively large sampling time (T_s=1 hour), which limits the sensitivity of the control action to changes in the energy weighting.

  Another possible explanation is that the energy factor affects only the control effort weighting (R) and is not involved in the temperature tracking cost (qT).

6.2.4 Overly Stringent Constraints

- **Action-1**: The simulation is executed using the default parameter values specified except that the constraint type is set to Constraint_Type = 0 (hard constraint) via the graphical user interface (GUI).
- **Observation-1**: MPC issues the warning "*Warning: The constraints are overly stringent. No feasible solution. Previous optimal sequence will be used*". Although the simulation continues to run, the resulting control actions and system trajectories are not reliable due to infeasibility.

- Note: To emulate hard-constraint-like behavior while maintaining numerical feasibility, it is recommended to use soft constraints with a sufficiently large constraint violation penalty (*e.g.*, *ECR_factor = 10^4*).

6.3 Humidity Tracking Tests

6.3.1 Insufficient HVAC power

- **Action-1**: The simulation is executed using the default parameter values specified through the graphical user interface (GUI).
- **Observation-1**: At the beginning of the simulation, the HVAC system actively operates in humidification mode, increasing the indoor humidity ratio to approximately 0.009. During the initial period, up to around hour 7, the humidity-disturbing terms—namely internal latent gains (Qlatent_int), ventilation-related latent exchange (Qlatent_vent), and infiltration-related latent exchange (Qlatent_inf) are inactive. As a result, the indoor humidity remains nearly constant during this interval.

  After hour 7:00, these latent disturbance terms become active. Occupant-related latent gains tend to increase the indoor humidity, whereas ventilation and infiltration introduce dry outdoor air and therefore act as moisture-removing mechanisms. Under the combined influence of these competing effects, the indoor humidity ratio begins to decrease.

  When the indoor humidity approaches the lower comfort limit (w_{min}), the HVAC system attempts to increase the humidity and drive it toward the reference value (w_{ref}). However, due to HVAC constraint limits, the controller is unable to further increase the humidity beyond the admissible range. Consequently, the indoor humidity remains bounded near the lower comfort threshold (**Figure 6.5**).

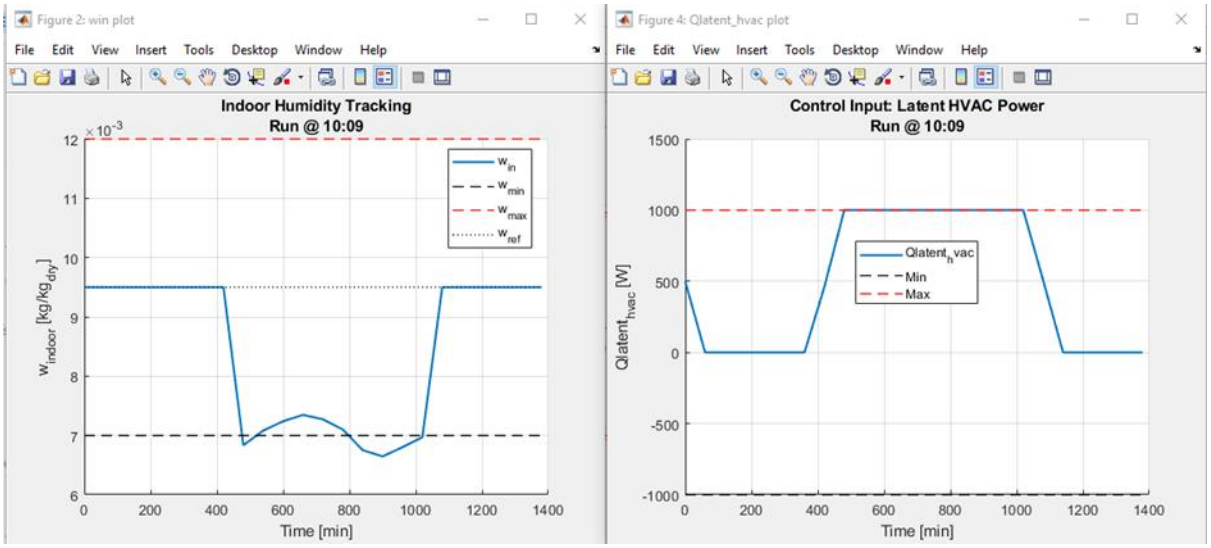

Figure 6-5 Humidity Tracking - Insufficient HVAC Power

6.3.2 Sufficient HVAC Power

- **Action-1**: The simulation is repeated after increasing the HVAC latent heating capacity to *Qsensible_hvac = 3000 W* via the GUI in order to evaluate whether the increased heating capacity can compensate for the observed humidity discomfort.
- **Observation-1**: The slight humidity drop is successfully compensated, and w*in* remains within the predefined comfort range throughout the entire simulation period. This result confirms that the previously observed humidity comfort violation was caused by insufficient HVAC sensible heating capacity rather than limitations in the MPC formulation or tuning parameters, thereby demonstrating the adequacy of the controller when sufficient HVAC power is available (**Figure 6.6**).

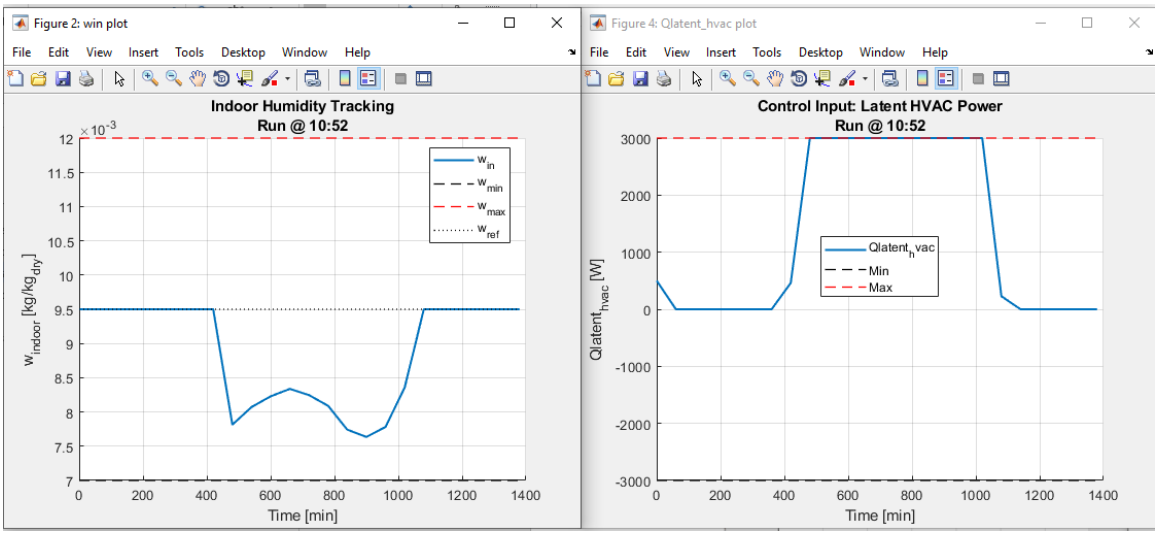

Figure 6-6 Humidity Tracking- Sufficient HVAC Power

6.3.3 Impact of the Cost Function on Humidity Tracking Test

- **Action-1** (***comfort cost test***) : Since the comfort factor affects only the temperature tracking cost and has no impact on the humidity control formulation, this test is not applicable to the humidity control case.
- **Action-2** (***control cost test***): The simulation is executed using the default parameter values, except for the comfort and energy factors. Since the adopted cost function is temperature-dominant, temperature tracking must first be relaxed by reducing the comfort factor to *comfort_factor = 0.01* before increasing the energy factor. Subsequently, the energy factor is significantly increased (e.g., *Energy_Factor = 10^6*) via the graphical user interface (GUI), and the simulation is re-executed.
- **Observation-2**: Slight drops are observed in the Q_{latent_hvac} trajectory following the adjustment of the cost weighting parameters (**Figure 6.7**).

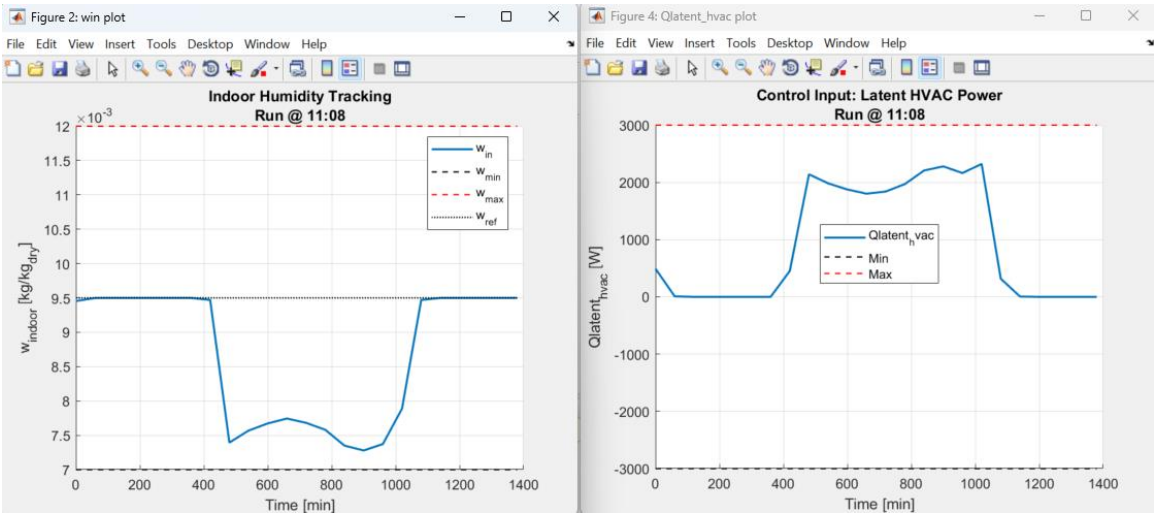

Figure 6-7 Impact of the Cost Function on Humidity Tracking

7 CONCLUSION

This study presented an extended aggregate thermal modeling framework that explicitly incorporates humidity-, ventilation-, and infiltration-induced thermal loads, as well as the additional thermal mass associated with furnishings within the case study building—effects that are commonly neglected in similar modeling approaches.

Simulation results highlight several important findings. First, the choice of sampling time was shown to have a significant impact on the interpretability of model behavior. A sampling time of Ts = 1 hour was found to be insufficient to fully capture the system's dynamic characteristics. Based on the observed dynamics and typical building thermal time constants, it can be inferred that a finer temporal resolution, such as Ts = 15 minutes (4 × 24-step daily horizon), would provide a more informative basis for evaluating thermal and humidity dynamics.

Second, under varying external disturbances, the model demonstrated the expected temperature and humidity tracking performance. The corresponding evolution of the cost function was consistent with the observed control actions, indicating coherent interaction between model dynamics, controller objectives, and imposed constraints.

Finally, the ability to perform simulations using user-adjustable parameters enables systematic exploration of system behavior and control sensitivity. From this perspective, the framework can be considered to support the objective of serving as an educational and learning-oriented tool.

REFERENCES

ASHRAE. (2017). *Handbook Fundamentals.*

Bergman, T. L. (2017). *Fundamentals of Heat and Mass Transfer* (8 ed.).

Boodi, A. (2022). *On Energy-Efficient Buildings Hybrd Dynamic Modelling for Analysis and Control.*

Boodi, A., Beddiar, K., Amirat, Y., & Benbouzid, M. (2022). *Building Thermal-Network Models: A Comparative Analysis,Recommendations, and Perspectives.*

Çengel, Y. A. (2020). *Heat and Mass Transfer Fundamentals and Applications.*

ISO, 5. (2017). *Energy performance of buildings – Energy needs for heating and cooling, internal temperatures and sensible and latent heat loads.*

ISO, 6. (2017). *Building components and building elements-Thermal resistance and thermal transmitence-Calculation methods.*

Michilidis, I., Michilidis, P., Minelli, F., & Coban, H. (2025). *Model Predictive Control for Smart Buildings: Applications and Innovation in Energy Management.*

S, K. (2012). *Thermal modelling of the building and its HVAC system using Matlab/Simulink.*

Taufiqoh, A. F. (2024). *INVESTIGATION OF RC MODELS FOR TEMPERATURE PREDICTION IN RESIDENTIAL ROOMS.*

Tayler , P., & Tarek, R. (n.d.). *Modeling of transient conduction in building envelope.*

APPENDICES

Appendix-1 Simulation GUI Views

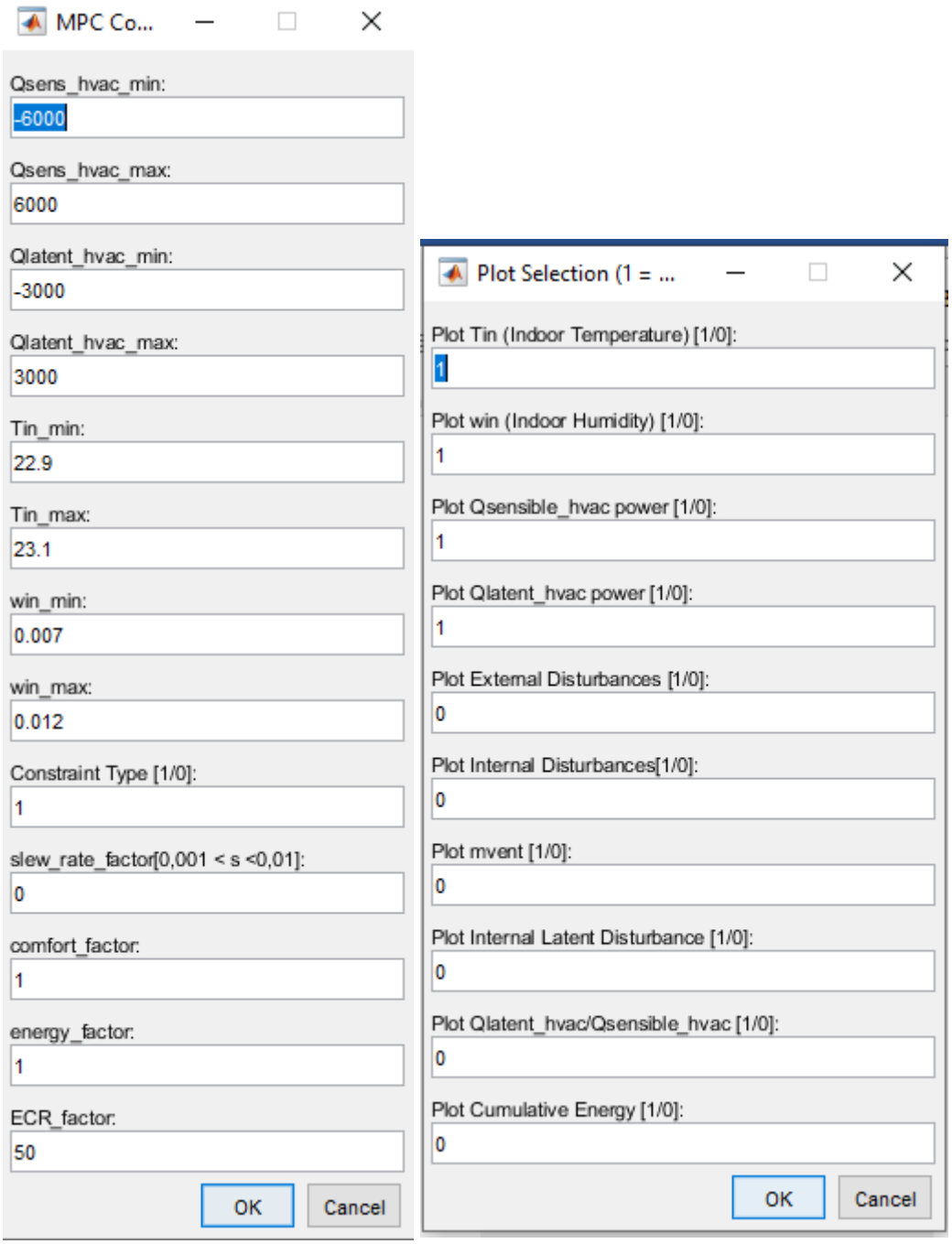

Figure Appendix 1 Simulation GUI Screen

Appendix-2 Model Parameterization Examples

Open Space
EPS Insulation
concrete
Gypsum Board
lab

Window/ Wall %	0,3000
width (m)	8,0000
Lenghth (m)	10,0000
Height (m)	3,0000
Anet (m^2)	24,0000

EPS Insulation	Combined Heat Transfer Coefficient (W/m^2.°K)	h1	21,1300
	Thickness (m)	L1	0,0800
	Thermal Conductivity (W/(m°C)	k1	0,0360
	Density (kg/$m^{3)}$	ρ1	20,0000
	Specific Heat (J/kg.°C)	cp1	1400,0000
	Surface Heat Transfer Coefficient (W/m2.°K)	hc	16,0000
	Radiative Heat Transfer Coefficient (W/m2.°K)	hr	5,1300
Concrete	Thickness (m)	L2	0,2000
	Thermal Conductivity (W/(m°C)	k2 (m)	1,7000
	Density (kg/m3)	ρ2 (kg/m3)	2300,0000
	Specific Heat (J/kg.°C)	cp2	880,0000
Gypsum Board	Surface Heat Transfer Coefficient (W/m2.°C)	h3	7,0900
	Thickness (m)	L3	0,0125
	Thermal Conductivity (W/(m°C)	k3 (m)	0,1600
	Density (kg/m3)	ρ3 (kg/m3)	900,0000
	Specific Heat (J/kg.°C)	cp3	840,0000
	Surface Heat Transfer Coefficient (W/m2.°C)	hc	2,5000
	Surface Heat Transfer Coefficient (W/m2.°K)	hr	4,5900

5R3C							
L1			L2		L3		
1/hA	ρALc_p	L/kA	ρALc_p	L/kA	ρALc_p	L/kA	1/hA
RcnvL1	CL1	RcndL1	CL2	RcndL2	CL3	RcndL3	RcnvL3
0,001972	53.760,00	0,092593	9.715.200,00	0,004902	226.800,00	0,003255	0,005877

2R1C		
Rew31	Rew32	Cew3
0,054299	0,054299	9.995.760,00

Figure Appendix 2 North Wall Parameterization

Open Space
EPS Insulation
concrete
Gypsum Board
lab

Window/ Wall %	0,3000
width (m)	8,0000
Lenghth (m)	10,0000
Height (m)	3,0000
Anet (m^2)	30,0000

EPS Insulation	Combined Heat Transfer Coefficient (W/m^2.°C)	h1	21,1300
	Thickness (m)	L1	0,0800
	Thermal Conductivity (W/(m°C)	k1	0,0360
	Density (kg/$m^{3)}$	ρ1	20,0000
	Specific Heat (J/kg.°C)	cp1	1400,0000
	Surface Heat Transfer Coefficient (W/m2.°C)	hc	16,0000
	Radiative Heat Transfer Coefficient (W/m2.°K)	hr	5,1300
Concrete	Surface Heat Transfer Coefficient (W/m2.°C)	h2	NA
	Thickness (m)	L2	0,2000
	Thermal Conductivity (W/(m°C)	k2 (m)	1,7000
	Density (kg/m3)	ρ2 (kg/m3)	2300,0000
	Specific Heat (J/kg.°C)	cp2	880,0000
Gypsum Board	Surface Heat Transfer Coefficient (W/m2.°C)	h3	7,0900
	Thickness (m)	L3	0,0125
	Thermal Conductivity (W/(m°C)	k3 (m)	0,1600
	Density (kg/m3)	ρ3 (kg/m3)	900,0000
	Specific Heat (J/kg.°C)	cp3	840,0000
	Surface Heat Transfer Coefficient (W/m2.°C)	hc	2,5000
	Radiative Heat Transfer Coefficient (W/m2.°K)		4,5900

5R3C							
L1			L2		L3		
1/hA	ρALc_p	L/kA	ρALc_p	L/kA	ρALc_p	L/kA	1/hA
RcnvL1	CL1	RcndL1	CL2	RcndL2	CL3	RcndL3	RcnvL3
0,001578	67.200,00	0,074074	12.144.000,00	0,003922	283.500,00	0,002604	0,004701

2R1C		
Rew21	Rew22	Cew2
0,043439	0,043439	12.494.700,00

Figure Appendix 3 West Wall Parameterization

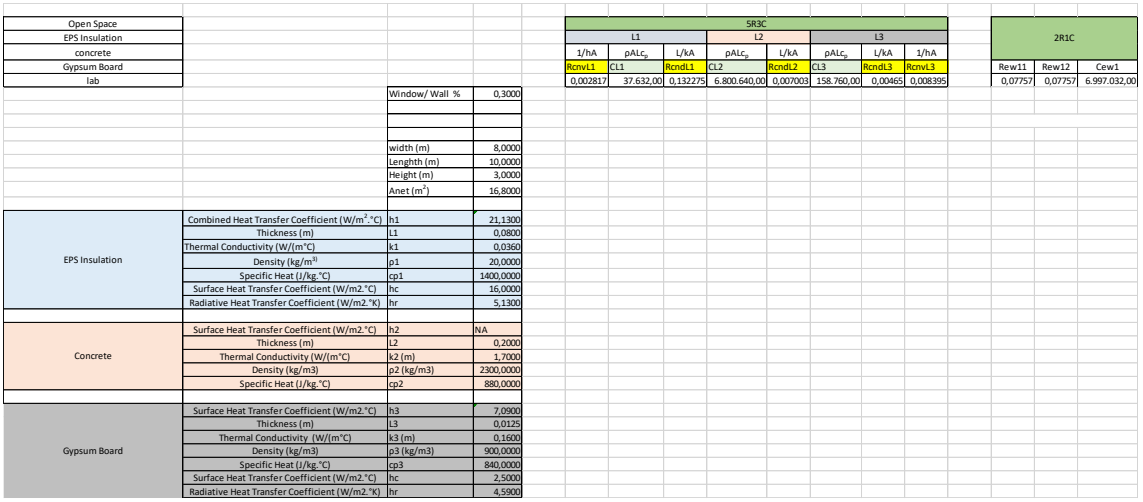

Open Space								5R3C																
EPS Insulation								L1			L2			L3						2R1C				
concrete								1/hA	ρALc$_p$	L/kA	ρALc$_p$	L/kA	ρALc$_p$	L/kA	1/hA									
Gypsum Board								RcnvL1	CL1	RcndL1	CL2	RcndL2	CL3	RcndL3	RcnvL3					Rew11	Rew12	Cew1		
lab								0,002817	37.632,00	0,132275	6.800.640,00	0,007003	158.760,00	0,00465	0,008395					0,07757	0,07757	6.997.032,00		
			Window/ Wall %	0,3000																				
			width (m)	8,0000																				
			Lenghth (m)	10,0000																				
			Height (m)	3,0000																				
			Anet (m^2)	16,8000																				
EPS Insulation	Combined Heat Transfer Coefficient (W/m^2.°C)	h1	21,1300																					
	Thickness (m)	L1	0,0800																					
	Thermal Conductivity (W/(m°C)	k1	0,0360																					
	Density (kg/m^3)	ρ1	20,0000																					
	Specific Heat (J/kg.°C)	cp1	1400,0000																					
	Surface Heat Transfer Coefficient (W/m2.°C)	hc	16,0000																					
	Radiative Heat Transfer Coefficient (W/m2.°K)	hr	5,1300																					
Concrete	Surface Heat Transfer Coefficient (W/m2.°C)	h2	NA																					
	Thickness (m)	L2	0,2000																					
	Thermal Conductivity (W/(m°C)	k2 (m)	1,7000																					
	Density (kg/m3)	ρ2 (kg/m3)	2300,0000																					
	Specific Heat (J/kg.°C)	cp2	880,0000																					
Gypsum Board	Surface Heat Transfer Coefficient (W/m2.°C)	h3	7,0900																					
	Thickness (m)	L3	0,0125																					
	Thermal Conductivity (W/(m°C)	k3 (m)	0,1600																					
	Density (kg/m3)	ρ3 (kg/m3)	900,0000																					
	Specific Heat (J/kg.°C)	cp3	840,0000																					
	Surface Heat Transfer Coefficient (W/m2.°C)	hc	2,5000																					
	Radiative Heat Transfer Coefficient (W/m2.°K)	hr	4,5900																					

Figure Appendix 4 South Wall Parameterization

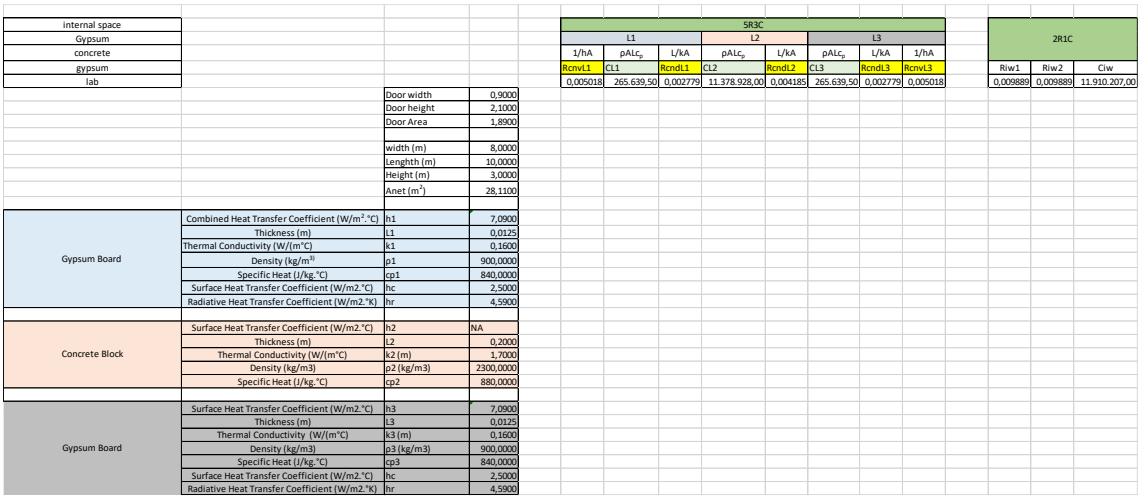

internal space								5R3C																
Gypsum								L1			L2			L3						2R1C				
concrete								1/hA	ρALc$_p$	L/kA	ρALc$_p$	L/kA	ρALc$_p$	L/kA	1/hA									
gypsum								RcnvL1	CL1	RcndL1	CL2	RcndL2	CL3	RcndL3	RcnvL3					Riw1	Riw2	Ciw		
lab								0,005018	265.639,50	0,002779	11.378.928,00	0,004185	265.639,50	0,002779	0,005018					0,009889	0,009889	11.910.207,00		
			Door width	0,9000																				
			Door height	2,1000																				
			Door Area	1,8900																				
			width (m)	8,0000																				
			Lenghth (m)	10,0000																				
			Height (m)	3,0000																				
			Anet (m^2)	28,1100																				
Gypsum Board	Combined Heat Transfer Coefficient (W/m^2.°C)	h1	7,0900																					
	Thickness (m)	L1	0,0125																					
	Thermal Conductivity (W/(m°C)	k1	0,1600																					
	Density (kg/m^3)	ρ1	900,0000																					
	Specific Heat (J/kg.°C)	cp1	840,0000																					
	Surface Heat Transfer Coefficient (W/m2.°C)	hc	2,5000																					
	Radiative Heat Transfer Coefficient (W/m2.°K)	hr	4,5900																					
Concrete Block	Surface Heat Transfer Coefficient (W/m2.°C)	h2	NA																					
	Thickness (m)	L2	0,2000																					
	Thermal Conductivity (W/(m°C)	k2 (m)	1,7000																					
	Density (kg/m3)	ρ2 (kg/m3)	2300,0000																					
	Specific Heat (J/kg.°C)	cp2	880,0000																					
Gypsum Board	Surface Heat Transfer Coefficient (W/m2.°C)	h3	7,0900																					
	Thickness (m)	L3	0,0125																					
	Thermal Conductivity (W/(m°C)	k3 (m)	0,1600																					
	Density (kg/m3)	ρ3 (kg/m3)	900,0000																					
	Specific Heat (J/kg.°C)	cp3	840,0000																					
	Surface Heat Transfer Coefficient (W/m2.°C)	hc	2,5000																					
	Radiative Heat Transfer Coefficient (W/m2.°K)	hr	4,5900																					

Figure Appendix 5 Internal Wall Parameterization

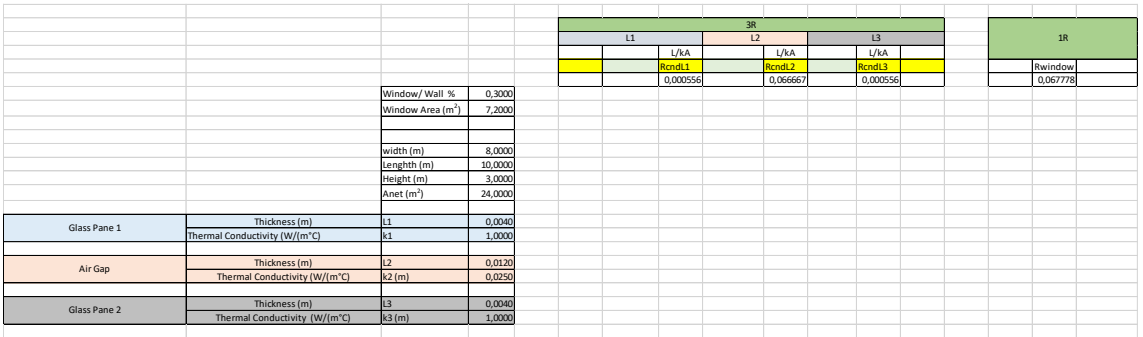

								3R																
								L1			L2			L3						1R				
										L/kA		L/kA		L/kA										
										RcndL1		RcndL2		RcndL3							Rwindow			
										0,000556		0,066667		0,000556							0,067778			
			Window/ Wall %	0,3000																				
			Window Area (m^2)	7,2000																				
			width (m)	8,0000																				
			Lenghth (m)	10,0000																				
			Height (m)	3,0000																				
			Anet (m*)	24,0000																				
Glass Pane 1	Thickness (m)	L1	0,0040																					
	Thermal Conductivity (W/(m°C)	k1	1,0000																					
Air Gap	Thickness (m)	L2	0,0120																					
	Thermal Conductivity (W/(m°C)	k2 (m)	0,0250																					
Glass Pane 2	Thickness (m)	L3	0,0040																					
	Thermal Conductivity (W/(m°C)	k3 (m)	1,0000																					

Figure Appendix 6 Window Parameterization

			1R								1R		
			L1			L2		L3					
					L/kA								
					RcndL1							Rdoor	
					0,151172							0,151172	
	Door width (m)	0,9000											
	Door height (m)	2,1000											
	Door Area (m^2)	1,8900											
Thickness (m)	L1	0,0400											
Thermal Conductivity (W/(m°C)	k1	0,1400											

Figure Appendix 7 Door Parameterization

					5R3C								2R1C		
ceramic/ stone tile					L1			L2		L3					
concrete					1/hA	ρALc_p	L/kA	ρALc_p	L/kA	ρALc_p	L/kA	1/hA			
mineral wool					RcnvL1	CL1	RcndL1	CL2	RcndL2	CL3	RcndL3	RcnvL3	Rf1	Rf2	Cf
lower floor (basement)					0,001303	1.344.000,00	0,000119	24.288.000,00	0,001103	100.800,00	0,015625	0,001303	0,009727	0,009727	25.732.800,00
			Window-Area (m2)	0,00											
			Door-Area (m2)	0,00											
			width (m)	8,00											
			Lenghth (m)	10,00											
			Height (m)												
			Anet (m^2)	80,00											
ceramic/ stone tail	Combined Heat Transfer Coefficient ($W/m^2.°C$)		h1	9,59											
	Thickness (m)		L1	0,01											
	Thermal Conductivity (W/(m°C)		k1	1,05											
	Density (kg/m^3)		ρ1	2000,00											
	Specific Heat (J/kg.°C)		cp1	840,00											
	Surface Heat Transfer Coefficient (W/m2.°C)		hc	5,00											
	Radiative Heat Transfer Coefficient (W/m2.°C)		hr	4,59											
	Thickness (m)		L2	0,15											
	Thermal Conductivity (W/(m°C)		k2 (m)	1,70											
	Density (kg/m3)		ρ2 (kg/m3)	2300,00											
	Specific Heat (J/kg.°C)		cp2	880,00											
Mineral Wool (insulation)	Combinedt Transfer Coefficient (W/m2.°C)		h3	9,59											
	Thickness (m)		L3	0,05											
	Thermal Conductivity (W/(m°C)		k3 (m)	0,04											
	Density (kg/m3)		ρ3 (kg/m3)	30,00											
	Specific Heat (J/kg.°C)		cp3	840,00											
	Surface Heat Transfer Coefficient (W/m2.°C)		hc	5,00											
	Radiative Heat Transfer Coefficient (W/m2.°C)		hr	4,59											

Figure Appendix 8 Floor Parameterization

					5R3C								2R1C		
					L1			L2		L3					
					1/hA	ρALc_p	L/kA	ρALc_p	L/kA	ρALc_p	L/kA	1/hA			
					RcnvL1	CL1	RcndL1	CL2	RcndL2	CL3	RcndL3	RcnvL3	Rc1	Rc2	Cc
					0,002363	725760	0,000938	201600	0,03125	32384000	0,001667	0,002363	0,01929	0,01929	33311360
			Window-Area (m2)	0											
upper floor			Door-Area (m2)	0											
concrete															
mineral wool															
gypsum lab			width (m)	8											
			Lenghth (m)	10											
			Height (m)												
			Anet (m^2)	80											
Gypsum Board	Surface Heat Transfer Coefficient ($W/m^2.°C$)		h1	5,29											
	Thickness (m)		L1	0,01											
	Thermal Conductivity (W/(m°C)		k1	0,16											
	Density (kg/m^3)		ρ1	900,00											
	Specific Heat (J/kg.°C)		cp1	840,00											
	Surface Heat Transfer Coefficient (W/m2.°C)		hc	0,70											
	Radiative Heat Transfer Coefficient (W/m2.°C)		hr	4,59											
	Thickness (m)		L2	0,10											
	Thermal Conductivity (W/(m°C)		k2 (m)	0,04											
	Density (kg/m3)		ρ2 (kg/m3)	30,00											
	Specific Heat (J/kg.°C)		cp2	840,00											
Concrete Slab	Surface Heat Transfer Coefficient (W/m2.°C)		h3	5,29											
	Thickness (m)		L3	0,20											
	Thermal Conductivity (W/(m°C)		k3 (m)	1,50											
	Density (kg/m3)		ρ3 (kg/m3)	2300,00											
	Specific Heat (J/kg.°C)		cp3	880,00											
	Surface Heat Transfer Coefficient (W/m2.°C)		hc	0,70											
	Radiative Heat Transfer Coefficient (W/m2.°C)		hr	4,59											

Figure Appendix 9 Ceiling Parameterization

				1R1C		
				Rm1	Rm2 (K/W)	Cm_{total} (J/K)
					0,000881523	510560
Combined Heat Transfer Coefficient ($W/m^2.°C$)	h1	7,09				
Surface Heat Transfer Coefficient (W/m2.°C)	hc	2,50				
Radiative Heat Transfer Coefficient (W/m2.°C)	hr	4,59				
Effective (approximated) heat transfer area of the internal content (furniture) coefficient (Y)		2				
Effective (approximated) heat transfer area of the internal content (furniture) (m^2) (Aeffective=Afloor*Y)		160				

Figure Appendix 10 Internal Mass Parameterization

Cc	Cf	Rwindow	Rdoor	Rew11	Rew12	Rew21	Rew22
3,33E+07	2,57E+07	0,067777778	0,15	0,07757036	0,07757036	0,043439401	0,043439401
Rew31	Rew32	Riw1	Riw2	Rm1	Rm2	Rc1	Rc2
0,054299252	0,054299252	0,009889443	0,009889443	0	0,000881523	0,019290032	0,019290032
Rf1	Rf2						
0,009726935	0,009726935						

Figure Appendix 11 RC Parameters

Appendix-3 Scenario

QSolar	SHGC	0,74	Qsolarwin=DirFactor*GTI*SHGC*Awin
	Awin (m^2) (south)	7,2	
	Aew1 (m^2) (south)	16,8	QsolarWall=DirFactor*GTI*Awall*α
	Aew2 (m^2) (west)	30	
	Aew3 (m^2) (north)	24	
	α (Solar Absorbance)	0,26	
	DirFactorNorth	0,2	Orientation Factor
	DirFactorWest	0,6	
	DirFactorSouth	0,9	

Figure Appendix 12 Qsolar Settings

						3105,2364	3105,2364	7763,091	3108,8004	3119,656	3119,656	7799,14	3120,052	88	88	220	88
		latent	Sensible Total		latent total	Qsens_int_ conv EWR	Qsens_int_ conv LuWR	Qsens_int_ conv WR	Qsens_int_ conv LaWR	Qsens_int_ rad EWR	Qsens_int_ rad LuWR	Qsens_int_ rad WR	Qsens_int_ rad LaWR	Qlatent EWR	Qlatent LuWR	Qlatent WR	Qlatent LaWR
			conductive	radiative													
People	man	55	63	87	110												
	woman	55	63	87	110												
		Totals	126	174	220	50,4	50,4	126	50,4	69,6	69,6	174	69,6	88	88	220	88
		nbr	Total QlabConv_light	Total QlabRad													
Lighting	Space Fraction	16	7215,936	7510,464		2886,3744	2886,3744	7215,936	2886,3744	3004,1856	3004,1856	7510,464	3004,1856				
	Radiative Fraction																
	LPD																
	Afloor (8*10)																
	Fsa (for LED)																
	Ful																
		Total Qconv	Total Qrad														
Office Equipments	laptop	110,4	36,8														
	laptop conv factor																
	monitor	74,88	49,92														
	monitor conv factor																
	desktop	167,04	18,56														
	desktop conv factor																
	common diversity factor																
	printer	9,345	4,005														
	printer conv factor																
	printer diversity factor																
	paper shredder	23,85	1,431														
	shredder conv factor																
	shredder diverity factor																
	aaa	0	0														
	aaa conv factor																
	aaa diversity factor																
	bbb	0	0														
	bbb conv factor																
	bbb diversity factor																
	ccc	0	0														
	ccc conv factor																
	ccc diversity factor																
		385,515	110,716			154,206	154,206	385,515	154,206	44,2864	44,2864	110,716	44,2864				
		Total Qconv	Total Qrad														
Lab Equipments	Function Generator	15,12	1,68														
	FG conv factor																
	FG diversity factor																
	Oscilloscope	20,52	2,28														
	Osc conv factor																
	Osc diversity factor																
	ddd	0	0														
	ddd conv factor																
	ddd diversity factor																
	eee	0	0														
	eee conv factor																
	eee diversity factor																
		35,64	3,96			14,256	14,256	35,64	17,82	1,584	1,584	3,96	1,98				

Figure Appendix 13 Internal Sensible-Radiant and Latent Heat Loads

7-8	Early Working Rate	0,4
12-13	Lunch Time Working Rate	0,4
8-12 /13-17	Working Rate	1
17-18	Late Working Rate	0,4
7-8	Early Lighting Rate	0,4
12-13	Lunch Time Lighting Rate	0,4
8-12 /13-17	Working Rate	1
17-18	Late Lighting Rate	0,4
7-8	Early Office Eq. Rate	0,4
12-13	Lunch Time Office Eq. Rate	0,4
8-12 /13-17	Working Rate	1
17-18	Late Office Eq. Rate	0,4
7-8	Early Lab Eq. Rate	0,4
12-13	Lunch Time Lab Eq. Rate	0,4
8-12 /13-17	Working Rate	1
17-18	Late Lab Eq. Rate	0,5

Figure Appendix 14 Internal Sensible-Radiant and Latent Configuration

ACH	0,5
$m_{\_inf}$ (kg/sec)	0,04

Figure Appendix 15 Infiltration Through Door Configuration

		ACH	m_{vent}
7-8	Early Working Rate	0,5	0,04
8-12 /13-17	Working Rate	10	0,8
17-18	Late Working Rate	7	0,56

Figure Appendix 16 Ventilation Configuration

Tfloor	Tceiling	QsolarWin	QsolarExWall1	QsolarExWall2	QsolarExWall3	Qsens_int_conv	Qsens_int_rad	m_inf	Q_latent_int	wfact	mvent	wout	sigma
16	16	0	0	0	0	0	0	0	0	0,0044	0,00	0,0052	0
16	16	0	0	0	0	0	0	0	0	0,0044	0,00	0,0053	0
16	16	0	0	0	0	0	0	0	0	0,0043	0,00	0,0061	0
16	16	0	0	0	0	0	0	0	0	0,0043	0,00	0,0061	0
16	16	0	0	0	0	0	0	0	0	0,0043	0,00	0,0060	0
16	16	0	0	0	0	0	0	0	0	0,0044	0,00	0,0059	0
16	16	0	0	0	0	0	0	0	0	0,0044	0,00	0,0059	0
18	18	0	0	0	0	3105,2364	3119,656	0,04	88	0,0045	0,04	0,0060	0,4
20	20	23,976	19,656	54	6,24	7763,091	7799,14	0,04	220	0,0046	0,80	0,0063	0,4
20	20	38,3616	31,4496	86,4	9,984	7763,091	7799,14	0,04	220	0,0046	0,80	0,0065	0,2
20	20	62,3376	51,1056	140,4	16,224	7763,091	7799,14	0,04	220	0,0047	0,80	0,0067	0,2
20	20	119,88	98,28	270	31,2	7763,091	7799,14	0,04	220	0,0047	0,80	0,0068	0,2
20	20	287,712	235,872	648	74,88	3105,2364	3119,656	0,04	88	0,0048	0,80	0,0068	0,5
20	20	148,6512	121,8672	334,8	38,688	7763,091	7799,14	0,04	220	0,0048	0,80	0,0065	0,2
20	20	513,0864	420,6384	1155,6	133,536	7763,091	7799,14	0,04	220	0,0048	0,80	0,0062	0,2
20	20	33,5664	27,5184	75,6	8,736	7763,091	7799,14	0,04	220	0,0049	0,80	0,0061	0,2
20	20	43,1568	35,3808	97,2	11,232	7763,091	7799,14	0,04	220	0,0049	0,80	0,0062	0,4
20	20	0	0	0	0	3108,8004	3120,052	0,04	88	0,0048	0,56	0,0063	0,4
20	20	0	0	0	0	0	0	0	0	0,0048	0,00	0,0062	0
18	18	0	0	0	0	0	0	0	0	0,0047	0,00	0,0062	0
16	16	0	0	0	0	0	0	0	0	0,0046	0,00	0,0063	0
16	16	0	0	0	0	0	0	0	0	0,0046	0,00	0,01	0
16	16	0	0	0	0	0	0	0	0	0,0045	0,00	0,01	0
16	16	0	0	0	0	0	0	0	0	0,0044	0,00	0,01	0

Figure Appendix 17 Scenario January

Appendix-4 MPC States Report for Test 6.2.2

Time_min	Tin_C	Tew1_C	Tew2_C	Tew3_C	Tiw_C	Tf_C	Tc_C	Tm_C	win_kgkg
0	23,00784383	17,93159149	17,93159149	17,93159149	18,03957282	18,01876004	18,00733688	22,70238459	0,0095
60	23,00744912	17,87610193	17,87610193	17,87610193	18,12445547	18,05993532	18,02364294	22,99297164	0,0095
120	23,00785093	17,835567	17,835567	17,835567	18,20602978	18,1007727	18,04009432	23,0052682	0,0095
180	23,00743945	17,79558271	17,79558271	17,79558271	18,28284037	18,14048744	18,05637633	23,00549947	0,0095
240	23,00697127	17,75480714	17,75480714	17,75480714	18,35509442	18,17907517	18,07247658	23,00517246	0,0095
300	23,00660359	17,71456787	17,71456787	17,71456787	18,42305934	18,2165665	18,08839657	23,00489749	0,0095
360	23,00629485	17,67551697	17,67551697	17,67551697	18,48699054	18,25299303	18,10413849	23,00467052	0,0095
420	23,00980614	17,63612564	17,63612564	17,63612564	18,59085985	18,30925276	18,12789481	25,65358467	0,0095
480	23,0014112	17,61370955	17,6191191	17,60589576	18,75004648	18,39330831	18,16293428	29,82494443	0,007814615
540	23,00141153	17,60580717	17,61980071	17,58559427	18,91277405	18,48123799	18,20005302	29,8734081	0,008071793
600	23,00140755	17,61204358	17,63991754	17,57178118	19,06600789	18,56674937	18,23678777	29,87401848	0,008228941
660	23,00145368	17,64428597	17,69884036	17,56548518	19,21015693	18,64983677	18,27311351	29,87405317	0,008336994
720	23,00164426	17,74996659	17,86871667	17,5784387	19,35856354	18,73674146	18,31147094	25,79665584	0,008247123
780	23,00138515	17,78892208	17,93964648	17,57120904	19,47262157	18,80886538	18,34453995	29,82638042	0,00808951
840	23,00193329	17,98091717	18,24541971	17,59885795	19,59248036	18,88500113	18,37963101	29,87347784	0,007741965
900	23,00106496	17,96687035	18,23546068	17,57890655	19,70545398	18,95908498	18,41437327	29,87428389	0,007635451
960	23,00101335	17,95439313	18,22918119	17,55747703	19,81173542	19,03107143	18,44872972	29,87432527	0,007782139
1020	23,00147075	17,92675688	18,19792382	17,5350713	19,92692775	19,10834664	18,48559545	25,81643228	0,008357867
1080	23,01272893	17,90050389	18,16809743	17,5139799	20,03693855	19,1842101	18,52235473	23,12492959	0,0095
1140	23,00489791	17,87102888	18,1350961	17,48959845	20,06520884	19,22191036	18,54454413	23,00889718	0,0095
1200	22,99744656	17,842434	18,10302138	17,46603001	20,03175842	19,22982715	18,55520256	22,99869376	0,0095
1260	22,99757314	17,8141958	18,07134919	17,44275202	20,00020179	19,23747626	18,56572519	22,99821402	0,0095
1320	22,99757422	17,78435232	18,03811697	17,41780338	19,97051319	19,24490693	18,57612996	22,99818498	0,0095
1380	22,99749118	17,75160727	18,00202784	17,38988866	19,94258333	19,25212609	18,58641849	22,99810746	0,0095

Figure Appendix 18 State Report for Test 6.2.2

Appendix-5 Simulation Result for Test 6.2.2

Time_min	Tout_C	wout_kgkg	QsolarWin_W	Qsens_int_conv_W	Qsens_int_rad_W	Qsens_vent_W	Qsens_inf_W	Qlatent_int_W	Qlatent_vent_W	Qlatent_inf_W	Qsensible_hvac_W	Qlatent_hvac_W	Tin_C	win_kgkg
0	4,3	0,005177575	0	0	0	0	0	0	0	0	2383,554505	500	23,00784383	0,0095
60	4,5	0,005251202	0	0	0	0	0	0	0	0	1883,57583	-1,97906E-09	23,00744912	0,0095
120	6,6	0,006082758	0	0	0	0	0	0	0	0	1821,757842	1,09139E-09	23,00785093	0,0095
180	6,6	0,006082758	0	0	0	0	0	0	0	0	1810,002629	9,09495E-11	23,00743945	0,0095
240	6,4	0,005992765	0	0	0	0	0	0	0	0	1802,644969	-9,09495E-11	23,00697127	0,0095
300	6,4	0,005932871	0	0	0	0	0	0	0	0	1792,981541	9,09495E-11	23,00660359	0,0095
360	6,5	0,005923859	0	0	0	0	0	0	0	0	1782,345075	-9,09495E-11	23,00629485	0,0095
420	6,9	0,006015514	0	3105,2364	3119,656	-648,258599	-80,63783959	88	-348,4486232	-200,44	-3586,619821	460,8886232	23,00980614	0,0095
480	7,8	0,006269764	23,976	7763,091	7799,14	-12234,09573	-48,31071461	220	-3089,703199	-130,4246045	-1542,297734	3000	23,0014112	0,007814615
540	8,6	0,006496321	38,3616	7763,091	7799,14	-11590,256	-24,15536002	220	-3150,942802	-69,03585631	-2332,095253	3000	23,00141153	0,008071793
600	9,2	0,006654377	62,3376	7763,091	7799,14	-11107,37279	-24,15532793	220	-3149,128134	-70,85882487	-2875,223337	3000	23,00140755	0,008228941
660	9,5	0,006763168	119,88	7763,091	7799,14	-10865,96992	-24,15569922	220	-3147,651159	-72,3398748	-3205,213335	3000	23,00145368	0,008336994
720	9,6	0,006790448	287,712	3105,2364	3119,656	-10785,6433	-60,39308256	88	-2913,35035	-174,6561639	5810,340644	3000	23,00164426	0,008247123
780	9,4	0,006512519	148,6512	7763,091	7799,14	-10946,39477	-24,15514773	220	-3153,982875	-66,03020396	-3134,890302	3000	23,00138515	0,00808951
840	9,1	0,006161151	513,0864	7763,091	7799,14	-11188,27591	-24,15955912	220	-3161,629533	-58,39930817	-3354,205326	3000	23,00193329	0,007741965
900	8,7	0,006053231	33,5664	7763,091	7799,14	-11509,49708	-24,15257082	220	-3164,439828	-55,56901126	-2570,785234	3000	23,00106496	0,007635451
960	8,3	0,006230647	43,1568	7763,091	7799,14	-11831,37555	-48,30431096	220	-3102,983329	-117,0055477	-2251,827143	3000	23,00101335	0,007782139
1020	8,2	0,00625362	0	3108,8004	3120,052	-8338,556561	-48,31167318	88	-2945,945896	-141,4346853	3511,429047	3000	23,00147075	0,008357867
1080	8,3	0,006216898	0	0	0	0	0	0	0	0	1256,148197	228,4265737	23,01272893	0,0095
1140	8,3	0,006209336	0	0	0	0	0	0	0	0	1440,886254	7,45058E-09	23,00489791	0,0095
1200	8,4	0,006291483	0	0	0	0	0	0	0	0	1457,943612	5,45697E-10	22,99744656	0,0095
1260	8,4	0,006483302	0	0	0	0	0	0	0	0	1462,387167	-1,69407E-21	22,99757314	0,0095
1320	8,1	0,006696103	0	0	0	0	0	0	0	0	1470,174803	-2,93649E-23	22,99757422	0,0095
1380	7,6	0,006492552	0	0	0	0	0	0	0	0	1480,830339	-2,93649E-23	22,99749118	0,0095

Figure Appendix 19 Test 6.2.2 Results